Applied Radiation and Isotopes 143 (2019) 47–59

Contents lists available at ScienceDirect

Applied Radiation and Isotopes

journal homepage: www.elsevier.com/locate/apradiso

A systematic review of clinical applications of polymer gel dosimeters in radiotherapy

Bagher Farhood[a], Ghazale Geraily[b,*], Seyed Mohammad Mahdi Abtahi[c,**]

[a] Department of Medical Physics and Radiology, Faculty of Paramedical Sciences, Kashan University of Medical Sciences, 8115187159 Kashan, Iran
[b] Medical Physics and Medical Engineering Department, Faculty of Medicine, Tehran University of Medical Sciences, Tehran, Iran
[c] Physics Department, Imam Khomeini International University, Qazvin, Iran

HIGHLIGHTS

- Most polymer gel dosimeters have acceptable dose accuracy.
- Acrylamide-based gel dosimeters are highly toxic.
- The dose response of methacrylic acid–based gel dosimeters is beam energy dependent.
- The sensitivity of *N*-isopropylacrylamide gel dosimeters is lower.
- It is difficult to judge which is the best polymer gel dosimeter to use in the clinic.

ARTICLE INFO

Keywords:
Polymer gel dosimetry
Clinical application
Radiotherapy
Brachytherapy
Neutron capture therapy

ABSTRACT

Radiotherapy has rapidly improved because of the use of new equipment and techniques. Hence, the appeal for a feasible and accurate three-dimensional (3D) dosimetry system has increased. In this regard, gel dosimetry systems are accurate 3D dosimeters with high resolution. This systematic review evaluates the clinical applications of polymer gel dosimeters in radiotherapy. To find the clinical applications of polymer gel dosimeters in radiotherapy, a full systematic literature search was performed on the basis of the Preferred Reporting Items for Systematic Reviews and Meta-Analyses (PRISMA) guidelines in electronic databases up to January 31, 2017, with use of search-related terms in the titles and abstracts of articles. A total of 765 articles were screened in accordance with our inclusion and exclusion criteria. Eventually, 53 articles were included in the study. The findings show that most clinical applications of polymer gel dosimeters relate to external radiotherapy. Most of the gel dosimeters studied have acceptable dose accuracy as a 3D dosimeter with high resolution. It is difficult to judge which is the best polymer gel dosimeter to use in a clinical setting, because each gel dosimeter has advantages and limitations. For example, methacrylic acid–based gel dosimeters have high dose sensitivity and low toxicity, while their dose response is beam energy dependent; in contrast, *N*-isopropylacrylamide gel dosimeters have low dose resolution, but their sensitivity is lower and they are relatively toxic.

1. Introduction

The purpose of radiotherapy is to cover the tumor tissue homogeneously with an adequate dose while minimizing the dose to the surrounding normal tissue (Mann et al., 2017; Tanha et al., 2014). At present, applied techniques in radiation oncology can deliver a dose distribution with high conformity and precision to the treatment target volume (Novotny et al., 2001). It is noteworthy that any error or inaccuracy in dose delivery during irradiation in these modern techniques can result in either an insufficient dose to the tumor tissue or a high dose to the adjacent vital organs (Abtahi et al., 2016). Hence, the determination of the three-dimensional (3D) dose distribution in a tissue-equivalent material, before radiotherapy, can decrease any possible error (Abtahi et al., 2016).

To verify the dose distributions resulting from modern radiotherapy techniques, a dosimeter is needed to accurately measure 3D dose

* Correspondence to: Medical Physics and Medical Engineering Department, Faculty of Medicine, Tehran University of Medical Sciences, Postcode: 1417613151 Tehran, Iran.
** Corresponding author.
E-mail addresses: gh-geraily@sina.tums.ac.ir (G. Geraily), Sm.abtahi@sci.ikiu.ac (S.M.M. Abtahi).

https://doi.org/10.1016/j.apradiso.2018.08.018
Received 13 February 2018; Received in revised form 20 August 2018; Accepted 21 August 2018
Available online 23 August 2018
0969-8043/

distributions with high spatial resolution (Hilts et al., 2000). In clinical radiotherapy, the use of gel dosimeters can help in the high-resolution and precise verification of 3D dose distributions obtained by treatment planning facilities, while most current dosimeters measure the dose in one or two dimensions only (such as thermoluminescent dosimeters, ionization chamber–based dosimeters, and radiographic film–based dosimeters) (Senden et al., 2006). Polymer gel dosimeters are constructed from chemical materials that are sensitive to radiation and are polymerized as a function of the absorbed dose on irradiation (Abtahi et al., 2014). Radiation induces structural changes in the different polymer gel dosimeters that can affect their properties, such as variation in the proton nuclear magnetic resonance relaxation times, mass density, opacity, and elasticity (Senden et al., 2006). These characteristics can be read out by magnetic resonance imaging (MRI) (Maryanski et al., 1993), x-ray computed tomography (CT) (Hilts et al., 2000), optical scanning (Maryanski et al., 1996a), and ultrasonography (Mather et al., 2002). Gel dosimetry has advantageous properties that can simplify radiotherapy dosimetry, particularly in conditions in which conventional dosimeters cannot be used (Ibbott, 2004). These characteristics consist of the capability of measuring complex 3D dose distributions; radiological tissue equivalence; radiation direction independency; high spatial resolution; integration of dose during a treatment; etc. (Abtahi et al., 2014, 2016). In addition, gel dosimeters are relatively safe to fabricate and handle, although there are some toxic components, such as acrylamide, that must be applied with appropriate protection (Ibbott, 2004).

The applications of gel dosimeters include basic dosimetry such as depth dose, penumbra, and wedge profiles in different types of beams; dose distributions from various imaging procedures; dose distribution from different radiotherapy techniques, such as conformal therapy, intensity-modulated radiotherapy (IMRT), and stereotactic radiosurgery; dose distributions around various brachytherapy sources; and assessment of tissue heterogeneities such as bone and air.

In this systematic review, we study clinical application of polymer gel dosimeters in radiotherapy. In addition, we try to answer the following questions: What features of polymer gel dosimeters are important for clinical applications? What are the characteristics of different polymer gel dosimeters? What are the advantages and limitations of different polymer gel dosimeters relative to each other? What is the best polymer gel dosimeter to use in the clinic?

2. Methods

2.1. Search strategy

This systematic review was designed on the basis of the 2009 Preferred Reporting Items for Systematic Reviews and Meta-Analyses (PRISMA) guidelines (Moher et al., 2009). A literature search was conducted to assess all available studies in electronic databases, including Scopus, PubMed, Embase, and Web of Science, up to October 31, 2017, by use of the following search terms in titles and abstracts: “polymer gel”; and “radiation therapy” or “radiotherapy” or “external radiation therapy” or “external radiotherapy” or “brachytherapy” or “neutron capture therapy” or “NCT” or “BNCT”; and “BANANA” or “BANG” or “PAG” or “MAG” or “MAGIC” or “MAGAT” or “PAGAS” or “MAGAS” or “PAGAT” or “NIPAM” or “*N*-isopropylacrylamide” or “MAGIC-A” or “MAGIC-f” or “VIPAR” or “PABIG” or “LMD” or “PAM-PSGAT” or “PAGATUG” or “PVA-BAT.”

2.2. Study selection

Original articles were included that met the following inclusion criteria: (a) studies that used a combination of “polymer gel” and other search terms; (b) studies with full-text articles; (c) studies with adequate information; (d) studies in English. The exclusion criteria included (a) studies with unrelated abstracts, (b) studies with incomplete data on the clinical application of polymer gel dosimeters in radiotherapy, (c) studies presented as a poster, (d) letters to the editor, (e) editorials, and (f) review articles.

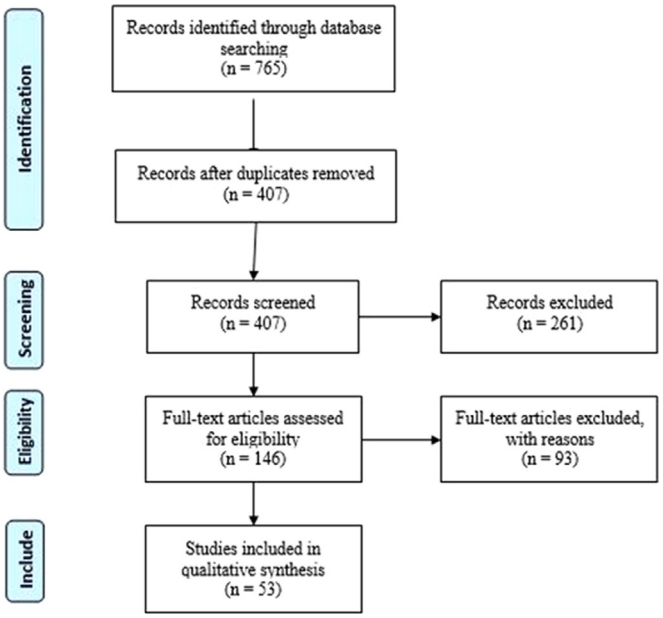

Fig. 1. Flowchart of the study selection process.

2.3. Data extraction

Each eligible article was reviewed, and the following information was extracted: (a) authors’ names; (b) polymer gel dosimeter type; (c) beam type (photon, electron, and/or neutron); (d) radiotherapeutic treatment type (external radiotherapy, brachytherapy, and/or boron neutron capture therapy [BNCT]); (e) clinical application type; (f) therapeutic technique type; (g) readout system type of the polymer gel dosimeter (MRI, optical CT, and/or x-ray CT); and (h) outcomes related to the use of polymer gel dosimeters in radiotherapy for clinical applications.

3. Results

3.1. Literature search

The study selection process is illustrated in Fig. 1.

Our initial search in the aforementioned databases up to November 1, 2017, identified 765 articles. After exclusion of duplicates, the numbers of articles were reduced to 407. After screening, 261 articles were excluded by checking the titles and abstracts of the articles, and 146 articles were qualified for full-text analysis. Then, studies with missing data or compliance studies with exclusion criteria were discarded. Finally, 53 articles were included in the systematic review. The extracted data and characteristics of the 53 articles are summarized in Table 1.

3.2. Clinical applications of polymer gel dosimeters

Different clinical applications of polymer gel dosimeters will be presented in three distinct sections, including external beam radiotherapy, brachytherapy, and BNCT. Because of the large number of studies, some are discussed in the following sections and the remaining studies not discussed are listed in Table 1.

3.2.1. External beam radiotherapy

Most clinical applications of polymer gel dosimeters relate to

Table 1
Characteristics of included studies.

Author and year	Gel type	Beam type	Treatment type	Technique type	Readout system	Clinical application
Oldham et al. (1998)	BANG	Photon	External	IMRT	MRI	Prostate
De Deene et al. (1998)	BANG	Photon	External	Conformal (non-IMRT)	MRI	Head and neck
Farajollahi et al. (1999)	BANG	^{137}Cs	Brachytherapy	–	MRI	Complex gynecological insertion
Hepworth et al. (1999)	BANG and PAG	Photon	External	Non-IMRT	MRI	Inhomogeneity (bone and air)
McJury et al. (1999)	PAG	^{192}Ir	Brachytherapy	–	MRI	Bronchus catheter
Meeks et al. (1999)	BANG	Photon	External	Stereotactic radiosurgery/ radiotherapy	MRI	Acoustic schwannomas
Cosgrove et al. (2000)	PAG	Photon	External	Stereotactic conformal	MRI	Benign tumor located in near the left eye and optic nerve
Chan et al. (2000)	BANG	^{106}Ru	Brachytherapy	–	MRI	Eye
Wojnecki and Green (2001)	PAG	Neutron	BNCT	–	MRI	Brain
Amin et al. (2003)	PAG	^{90}Sr/^{90}Y	Brachytherapy	Intravascular	MRI	Curved coronary artery
Wuu et al., (2002, 2003)	BANG	^{188}Re	Brachytherapy	Intravascular	Optical CT	Coronary vessel wall
Guillerminet et al. (2003)	PAG	Photon	External	Non-IMRT	MRI	Inhomogeneity (bone)
Gustavsson et al. (2003)	MAGIC	Photon	External	Non-IMRT	MRI	Kidney-shaped target
Kipouros et al. (2003)	VIPAR	^{192}Ir	Brachytherapy	Monotherapy	MRI	Prostate
Uusi-Simola et al. (2003)	BANG-3	Neutron	BNCT	–	MRI	Brain
Trapp et al. (2004)	MAGIC	Photon and electron	External	Non-IMRT and IMRT	MRI	Carcinoma of the scalp
Watanabe et al. (2004)	BANG-3	Photon	External	Stereotactic radiosurgery	MRI	Inhomogeneity (bone and air)
Xu et al. (2004)	BANG-3	Photon	External	Non-IMRT	Optical CT	Brain
Gifford et al. (2005)	MAGIC	^{137}Cs	Brachytherapy	Intracavity	MRI	Cervical cancer
Gambarini et al. (2006)	PAG	Neutron	BNCT	–	MRI	Liver
Ravichander et al. (2006)	PAGAT	Photon	External	Non-IMRT	MRI	Head and neck field matching
Wuu and Xu (2006)	BANG-3	Photon	External	IMRT	Optical CT	Small brain tumor
Lopatiuk-Tirpak et al. (2008)	BANG-3	Photon	External	Non-IMRT	Optical CT	Lung
Baker et al. (2009)	BANG-1	Photon	External	Non-IMRT	MRI	Ocular tumors
Kozicki et al. (2009)	VIPAR	Photon	External	Non-IMRT	MRI	Brain tumor
Marques et al. (2009)	MAGIC-f	^{192}Ir	Brachytherapy	–	MRI	Esophagus
Pourfallah et al. (2009)	PAGAT	Photon	External	Stereotactic radiosurgery	MRI	Inhomogeneity (bone and air)
Toossi et al. (2009)	MAGAT	Photon	External	Non-IMRT	MRI	Bladder cancer
Marques et al. (2010)	MAGIC-f	Photon	External	Non-IMRT	MRI	Gold nanoparticles
Gopishankar et al. (2012)	MAGAT	Photon	External	Stereotactic radiosurgery	MRI	Pituitary adenoma
Kairn et al. (2012)	PAGAT	Photon	External	Stereotactic radiotherapy	Optical CT	Meningioma
Pavoni et al. (2012)	MAGIC-f	Photon	External	Tomotherapy	MRI	Prostate
Fazli et al. (2013)	MAGIC-A	^{192}Ir	Brachytherapy	–	MRI	Nasopharynx
Gopishankar et al. (2013)	MAGAT	Photon	External	IMRT	MRI	Spinal metastasis target
Govi et al. (2013)	MAGAT	^{192}Ir	Brachytherapy	–	MRI	Breast balloon
Khadem-Abolfazli et al. (2013)	MAGIC-A	Photon	External	Non-IMRT	MRI	Gold nanoparticles
Chen et al. (2014)	NIPAM	Photon	External	IMRT	MRI	Eye
Da Silveira et al. (2014)	MAGIC-f	Photon	External	IMRT	MRI	Prostate
Deyhimihaghighi et al. (2014)	PAGAT	Photon	External	Non-IMRT	MRI	Platinum nanoparticles
Fuse et al. (2015)	BANG-Pro	Photon	External	Non-IMRT	MRI	Breast conserving therapy and bolus compensator
Kakade and Sharma (2015)	PAGAT	Photon	External	Non-IMRT	MRI	Prostate and gold nanoparticles
Cuevas et al. (2016)	MAGIC-f	Photon	External	IMRT	MRI	Prostate
Khosravi et al. (2015)	MAGIC-f	Photon and ^{192}Ir	External and brachytherapy	Non-IMRT	MRI	Prostate and gold nanoparticles
Cheng et al. (2016)	NIPAM	Photon	External	IMRT	MRI	Eye
Khosravi et al. (2016)	MAGIC-f	^{192}Ir	Brachytherapy	Non-IMRT	MRI	Prostate and gold nanoparticles
Bavarnegin et al. (2017)	NIPAM	Neutron	BNCT	–	MRI	Brain
Hsieh et al. (2017)	NIPAM	Photon	External	IMRT	MRI	Intracranial meningioma
Khajeali et al. (2017)	NIPAM	Neutron	BNCT	–	MRI	Shallow brain tumors
Ghaseminejad et al. (2017)	NIPAM	Photon	External	IMRT	MRI	Inhomogeneity (bone)
Mann et al. (2017)	PAGAT	Photon	External	Adaptive radiotherapy	MRI	Lung
Silveira et al. (2017)	MAGIC-f	Photon	External	IMRT	MRI	Prostate
Yao et al. (2017)	NIPAM	Photon	External	VMAT and IMRT	Optical CT	Lung and larynx

BNCT, boron neutron capture therapy; CT, computed tomography; IMRT intensity-modulated radiotherapy; MAGAT, methacrylic acid, gelatin, and tetrakis(hydroxymethyl)phosphonium chloride; MAGIC, methacrylic acid, ascorbic acid, gelatin, and copper; MAGIC-A, methacrylic acid, ascorbic acid, gelatin, copper, and agarose; MAGIC-f, methacrylic acid, ascorbic acid, gelatin, copper, and formaldehyde; MRI, magnetic resonance imaging; NIPAM, *N*-isopropylacrylamide; PAG, polyacrylamide gel; PAGAT, polyacrylamide, gelatin, and tetrakis(hydroxymethyl)phosphonium chloride; VIPAR, *N*-vinylpyrrolidone-argon; VMAT, volumetric modulated arc therapy.

external beam radiotherapy. With the advent of complex and precise radiotherapeutic techniques such as IMRT, volumetric modulated arc therapy (VMAT), and stereotactic radiosurgery, the demand for an accurate and feasible 3D dosimetry system such as a gel dosimeter has increased (Khezerloo et al., 2017).

In 1998, Oldham et al. used a BANG gel dosimeter for dosimetric evaluation of nine-field tomotherapy irradiation. This treatment planning simulated a prostate treatment. They found that the gel dosimeter provided good agreement with dose distributions predicted by a treatment planning system (TPS) at medium and high doses (50–90%

isodose), although differences were observed at lower doses (30% isodose) up to 10%. They concluded that the BANG gel dosimeter has the potential to verify IMRT dose distributions; however, considerable care is needed to achieve accurate results (Oldham et al., 1998). Cosgrove et al. assessed the reproducibility of a polyacrylamide gel (PAG) dosimeter in stereotactic conformal radiotherapy. The plans used in their study were three coplanar fields and four non-coplanar fields. The beam geometry of the second plan was used for treatment of a benign tumor located near the left eye and optic nerve. They reported the relative dose distributions can be reproducible, with the standard deviation on the mean regions with higher than the 50% isodose curves obtained in three orthogonal fields being 4.1% and 6.4% for the non-coplanar and coplanar fields, respectively. Furthermore, the measured dose distributions were in line with those calculated by the TPS. Finally, they concluded that despite the limitations of the PAG dosimetry technique, especially for calibration of dose distributions to absolute dose, it is capable of verifying complex conformal treatment plans (Cosgrove et al., 2000). Trapp et al. used a methacrylic acid, ascorbic acid, gelatin, and copper (MAGIC) gel dosimeter for verification of photon and electron treatment plans in carcinoma of the scalp. In electron fields, their findings showed that the gel and diode data were generally in good agreement, with a small difference in the buildup region. Also, for IMRT fields, the isodose contours generated by the TPS were in good agreement with those measured by the gel dosimeter. Finally, the results from this study demonstrate that the use of gel dosimetry has become a beneficial dosimetric tool in radiotherapy (Trapp et al., 2004). Ravichander et al. used a polyacrylamide, gelatin, and tetrakis (hydroxymethyl)phosphonium chloride (PAGAT) gel dosimeter for head and neck field matching verification. In this study, the full width at half maximum through the nondiverging orthogonal head and neck field junction was determined with film, the gel dosimeter, and the TPS. The full width at half maximum difference between the PAGAT polymer gel and the film was within 0.5 mm. Furthermore, the maximum difference between gel dosimeter and Pinnacle TPS profiles was 7%. They stated that these differences are related to several factors, such as the detector size used for calculation of the profiles in the Pinnacle TPS and CT voxel limitation (Ravichander et al., 2006). Kozicki et al. evaluated application of the VIPARnd-GeVero® tool in a brain tumor radiotherapy. In this study, the software program GeVero® was used to process polymer gel data obtained from MRI, and the findings were compared with the dose distribution calculated by the TPS. Their results showed satisfactory agreement between VIPARnd gel dosimetry and TPS dose distributions. In addition, the usefulness of GeVero® and the VIPARnd gel dosimeter was proved in radiotherapy dosimetry. It was also shown that this software facilitates data processing (Kozicki et al., 2009). Gopishankar et al. investigated the accuracy of a source plugging–based treatment plan in Gamma Knife stereotactic radiosurgery by using a methacrylic acid, gelatin, and tetrakis(hydroxymethyl)phosphonium chloride (MAGAT) gel dosimeter and EBT2 film. In this study, a Y-shaped target and two organs at risk on either side of the target were created; this beam geometry simulates a pituitary adenoma tumor with optic nerves on either side. For 80% and 50% isodose curves, there were distance agreements of 2 mm and 1 mm, respectively, between gel measurements and TPS calculations. Furthermore, the results related to 3D gamma index analysis demonstrated a more than 94% voxel pass rate for tolerance criteria of 2%/2 mm, 3%/1 mm, and 3%/2 mm. In conclusion, they suggested that a MAGAT gel dosimeter can be used for verification of plug-based treatment planning (Gopishankar et al., 2012). Kairn et al. verified the PAGAT gel dosimeter response in accurate, high-resolution, 3D dose measurements of stereotactic radiotherapy fields by using Monte Carlo simulations. In this study, a small cylindrical container was filled with the PAGAT gel and located in the parietal region within a heterogeneous head phantom and then irradiated with a 12-field, non-coplanar, conformal stereotactic radiotherapy plan. They copied this beam geometry from a meningioma patient plan. The dose distributions obtained from the gel measurement and Monte Carlo simulations were in better agreement with each other than with those calculated by pencil beam TPS. Both data sets (gel dosimeter and Monte Carlo simulations) demonstrated close agreement with the TPS calculations through the center of the irradiated volume. However, the dose distributions obtained from Monte Carlo simulations and the gel dosimeter had subtle dose variations and narrower beam penumbrae than those from TPS calculations. In conclusion, the Monte Carlo data allowed the accuracy of the PAGAT gel dosimeter to be verified, allowing the PAGAT gel dosimeter to be used in the measurement of the dose from stereotactic radiotherapy and other types of radiotherapy (Kairn et al., 2012). Gopishankar et al. used a multipurpose acrylic head phantom to verify IMRT planning by using MAGAT gel and film dosimetry. They delineated a planning target volume of a doughnut shape along with an inner organ at risk for IMRT planning, as this plan simulates a spinal metastasis target. For this purpose, a nine-field IMRT plan was designed with the Pinnacle TPS. Three-dimensional gamma index analysis between the measured gel dose and the calculated TPS dose demonstrated a higher than 90% voxel pass rate for tolerance criteria of 1%/1 mm and 2%/2 mm. Finally, they reported that gel dosimetry has the potential to extract 3D dosimetric data in routine clinical applications (Gopishankar et al., 2013). Silveira et al. compared the results of 3D dosimetry with a gel dosimeter based on MAGIC with formaldehyde added (MAGIC-f) with those of conventional quality assurance procedures of one- and two-dimensional dosimetry in prostate cancer IMRT planning. In this study, a gamma index of 3%/3 mm was used to compare the 3D measurements of the gel dosimeter and the dose distributions obtained from the TPS. The gel dosimetry findings agreed with those of the conventional quality control procedures. Finally, they concluded that a MAGIC-f gel dosimeter associated with MRI can be used to evaluate the dose distribution in 3D quality control. In addition, it allows volumetric analyses, providing data that cannot be obtained by conventional quality control (Silveira et al., 2017). Yao et al. verified the dose distribution of the VMAT technique for two simple and complex clinical cases by using an *N*-isopropylacrylamide (NIPAM) gel dosimeter. For the simple case of lung cancer, there were high gamma passing rates (between the gel dosimeter and the TPS) for both the IMRT technique and the VMAT technique. However, there were slightly lower gamma passing rates for the complex case of larynx cancer than for the simple case for both the IMRT technique and the VMAT technique (Yao et al., 2017).

Hepworth et al. investigated dose maps of inhomogeneities in BANG gel and PAG dosimeters. In this study, the high- and low-density inhomogeneities were designed to simulate the effects of bone and air cavities in the body, respectively, as well as their effects on the absorbed dose during radiotherapy. They stated that an intrinsic problem of the gel dosimeter is the inhibition of polymerization because of dissolved oxygen. Therefore, they reported that more care is required in the manufacture of gel dosimeters as well as in the preparation of the inhomogeneity (Hepworth et al., 1999). Watanabe et al. used a cylindrical phantom filled with BANG-3 gel to measure 3D dose distributions in inhomogeneous media (air gap and bone). In this study, the effects of MRI artifacts resulting from the presence of foreign material within the phantom filled with the gel were observed. They found that the geometric distortion of MRI is less than 2 mm. Their results showed that oxygen contamination and unintentional small air gaps in the gel dosimeter can lead to a measured absorbed dose error of as large as 10% near the interface between the gel dosimeter and the heterogeneity. They suggested that better quantification of MRI artifacts and further enhancement of the signal-to-noise ratio will help to decrease the uncertainty of measured dose distributions (Watanabe et al., 2004). Pourfallah et al. investigated the effects of the presence of inhomogeneities on differential dose volume histograms of single-shot irradiations with a Gamma Knife unit by using EGSnrc simulation and a PAGAT gel dosimeter. The results of measurement and simulation showed that there are some differences between these two for very high isodose levels. It seems that the discrepancies can be attributed to the

diffusion of monomers in these regions (i.e., 70–80% isodose levels) during gel irradiation and in the initial hours after irradiation. Nevertheless, their results demonstrated that the presence of bone and air inhomogeneities in irradiation with the Gamma Knife unit can lead to disturbances in the dose distribution and the PAGAT gel dosimeter is able to detect these disturbances (Pourfallah et al., 2009). Ghaseminejad et al. investigated the effect of bone heterogeneity on dose distribution of small IMRT beamlets using a NIPAM gel dosimeter and Monte Carlo simulation. Fairly close agreement was observed between the gel dosimeter and Monte Carlo data to within ± 3%. Moreover, their results showed that with dose fluctuations in the presence of bone heterogeneity, the NIPAM gel dosimeter is able to evaluate the dose variations at bony interfaces (Ghaseminejad et al., 2017).

Marques et al. analyzed the use of gold nanoparticles (AuNPs) in kilovoltage radiotherapy by gel dosimetry. AuNPs were embedded inside a MAGIC-f gel dosimeter and irradiated with a 250-kV x-ray clinical beam. The response of the MAGIC-f gel dosimeter to the beam was specified by comparison of experimental and Monte Carlo–simulated percentage depth dose curves. The MAGIC-f gel dosimeter showed a linear response in the dose range from 0 to 10 Gy. The findings demonstrated good agreement (97%) between the gel dosimeter measurements and simulated dose enhancements for all AuNP concentrations studied (0.02, 0.05, and 0.10 mM). Finally, they concluded that gel dosimetry can be considered a suitable tool for dosimetric evaluations of nanoparticle applications in radiotherapy (Marques et al., 2010). Khadem-Abolfazli investigated the dose-enhancement effect of AuNPs MAGIC with agarose (MAGIC-A) gel in megavoltage radiotherapy. Their findings showed that in the dose range from 0 to 600 cGy, the MAGIC-A gel dose response is linear and the dose resolution in this dose range is lower than 0.7 Gy. Furthermore, the MAGIC-A gel dosimeter response (R_2) was increased with the addition of AuNPs. Moreover, they reported that a shielding effect or self-absorption occurred at 0.2 and 0.4 mM (Khadem-Abolfazli et al., 2013). Deyhimihaghighi et al. evaluated the feasibility of using PAGAT gel combined with platinum nanoparticles (PtNPs) as a dose enhancer or dosimeter to increase the optical density in MRI. They embedded various concentrations of PtNPs inside the PAGAT gel dosimeter and irradiated it with ^{60}Co. Their findings showed that in the presence of PtNPs at a concentration of 1×10^{-2} mg/l, the optical density increased by a factor of 27.10% (Deyhimihaghighi et al., 2014). Khosravi et al. assessed the ability of a MAGIC-f gel dosimeter by Monte Carlo simulation and experimental measurement to study the effect of AuNPs in prostate dose distributions. Their data showed that when external 18-MV radiotherapy was used, the mean absorbed doses obtained with the gel dosimeter and Monte Carlo simulation in prostate and in the presence of the AuNPs were 8% and 7% higher, respectively, than those in the absence of AuNPs. Therefore, there was good agreement between the gel dosimeter measurements and the Monte Carlo simulations. In conclusion, they indicated that the gel dosimetry method can be used as a reliable technique for evaluating the dose-enhancement caused by AuNPs in external radiotherapy practices (Khosravi et al., 2015).

Fuse et al. used BANG-Pro gel as a dosimeter and a bolus compensator in the near-surface buildup region in breast-conserving therapy. The gel bolus is a water equivalent and can be constructed from different tissue compensators. Their results validated the usefulness of BANG-Pro gel bolus in the near-surface buildup region to improve treatment in the chest wall/whole breast (Fuse et al., 2015).

3.2.2. Brachytherapy

Brachytherapy is a type of radiotherapy in which one or many sealed radioactive sources are placed at short distances from a tumor. With this treatment modality, the tumor volume receives a high radiation dose, while there is rapid dose fall-off in the surrounding normal tissues (Khan and Gibbons, 2014). Gel dosimeters are able to acquire steep dose gradients in 3D, and this property makes them very attractive for obtaining the dose distributions around brachytherapy sources. Furthermore, these dosimeters integrate the dose delivery during the treatment time, and the total dose distribution resulting from a moving source can be measured (Baldock et al., 2010).

Chan et al. measured the 3D dose distribution of a ^{106}Ru ophthalmological applicator using a BANG gel dosimeter. In this study, an eye phantom made of the BANG gel was irradiated with the ^{106}Ru source for up to 1 h. Then isodoses and depth doses of the ^{106}Ru eye plaque were obtained. They suggested that the BANG gel dosimeter has the potential to measure the 3D dose distributions around an ophthalmological applicator with relatively good accuracy and high spatial resolution (Chan et al., 2000). Amin et al. measured dose profiles and orthogonal and radial dose distributions for a ^{90}Sr/^{90}Y source (beta emitters) using a PAG dosimeter and compared them with measurements made with radiochromic films. The phantom used in this study resembled a curved coronary artery. The findings indicated that the PAG dosimeter can be used to measure the dose distributions characterized by the American Association of Physicists in Medicine for vascular brachytherapy sources with high-resolution MRI (4.7 T). They stated that this technique is, however, limited to centers with high-resolution MRI. A further disadvantage of using a PAG dosimeter is that stringent methods must be used to exclude oxygen during the construction of the gel dosimeter (Amin et al., 2003). Kipouros et al. evaluated the capability of an *N*-vinylpyrrolidone-argon (VIPAR) gel dosimeter to provide 3D dose distribution verification in ^{192}Ir prostate monotherapy. Their findings showed that there are significant differences between the calculated and experimental 3D dose distributions for doses lower than 50% of the prescribed dose, which could be because of the limited dose resolution of the VIPAR gel–MRI method for this low dose gradient–low dose region. Furthermore, the measurements revealed distortions at distances extending 1–1.5 mm around each catheter because of susceptibility artifacts. However, for most remaining points, the deviations between the calculated and the corresponding measured data were within the adopted acceptance criterion of 5%/3 mm. In conclusion, they reported that the VIPAR gel–MRI procedure can be used for the experimental verification of the dose distribution in a brachytherapy application involving source dwell positions and/or multiple catheters (Kipouros et al., 2003). Gifford et al. compared Monte Carlo simulations around a Fletcher-Suit-Delclos ovoid with a MAGIC gel dosimeter and radiochromic film. This ovoid in intracavitary brachytherapy of cervical cancer has shields that lead to reduction of the dose to the rectum and bladder. The findings revealed that the MCNPX 2.5.c Monte Carlo code can calculate the dose distribution accurately in the presence of the ovoid shields, and that the radiochromic film and the MAGIC gel dosimeter can show the effect of ovoid shields on the dose distribution (Gifford et al., 2005). Marques et al. evaluated the response of a MAGIC-f gel dosimeter around a ^{92}Ir high-dose-rate (HDR) brachytherapy source. In this study, an esophageal catheter was used to guide the source. The results obtained with this gel dosimeter were compared with those from PENELOPE Monte Carlo simulations and ionization chamber measurements. There was a maximum difference of 3.10% between the Monte Carlo simulations and the gel dose measurements at a radial distance of 18 mm from the ^{92}Ir source. Furthermore, the data demonstrated that the response of the MAGIC-f gel dosimeter is strongly affected by the dose rate and that different calibration should be used for areas near the source as well as for areas with lower dose rates. Finally, they reported that the MAGIC-f gel dosimeter can be successfully used to obtain accurate dose distributions from HDR brachytherapy sources if the appropriate calibration is performed (Marques et al., 2009). Fazli et al. compared the dosimetric data between a TPS, a MAGIC-A gel dosimeter, and Monte Carlo simulation in a heterogeneous nasopharynx phantom for HDR brachytherapy. Their results revealed a predictable agreement between the data obtained with the MAGIC-A gel dosimeter and the MCNP5 Monte Carlo simulation, and discrepancies at different distances were between 5.7% and 7.4%. One of the reasons for these discrepancies could be due to the simplifications in Monte Carlo simulation, but the most important

reason could be practical errors in experimental dosimetry. In addition, the MAGIC-A gel dosimeter had better resistance against temperature increases; however, increase of the temperature is uncontrollable in HDR brachytherapy because of the high dose gradients close to the source. There was acceptable agreement between the data from the MAGIC-A gel dosimeter and the results from the TPS calculations, and discrepancies at different distances were between 5.2% and 9.4%. The sources of the discrepancies in this comparison could be related to the variation in the calculations and the practical errors in the experimental dosimetry (Fazli et al., 2013). Govi et al. specified the response of a MAGAT gel dosimeter for breast brachytherapy applications through two balloon applicators. The dose maps of balloons obtained from MRI were compared with the TPS data. The gel dosimetry results showed very good agreement (more than 95%) with the TPS data. Finally, they concluded that the MAGAT gel dosimeter can be used as a reliable tool for 3D dose verification in balloon brachytherapy techniques (Govi et al., 2013).

Khosravi et al. evaluated the effects of AuNPs on the dose distribution for prostate in brachytherapy using MAGIC-f gel dosimetry and Monte Carlo simulation. In this study, the tolerance criterion of 7%/7 mm was used to analyze the data obtained with the gel dosimeter and the Monte Carlo simulation, and high pass rates of 91.7% and 86.4% were achieved with and without AuNPs, respectively. The comparison of gel dose measurements with Monte Carlo calculation indicated good agreement, particularly in the region of the planning target volume. In conclusion, they reported that the MAGIC-f gel dosimeter could be recommended as a reliable tool for evaluating the dose enhancement caused by various concentrations of AuNPs in brachytherapy (Khosravi et al., 2016).

3.2.3. Boron neutron capture therapy

BNCT is a targeted radiotherapy based on the nuclear capture that occurs when ^{10}B (nonradioactive) is irradiated with thermal neutrons (energies less than 0.025 eV). Following the interaction, high linear energy transfer (LET) products (alpha particles and recoiling ^{7}Li nuclei) are produced (Farhood and Ghorbani, 2015; Khosroabadi et al., 2016). These products deposit their energies in the range of 5–9 μm, which corresponds to the diameter of a cell (Cerullo et al., 2004). Several studies have been conducted using gel dosimeters in BNCT dosimetry because of their advantages, such as the tissue equivalence of the gel dosimeter at these energies, and also its ability to separate the components of the dose (Ibbott, 2004).

Wojnecki et al. evaluated performance of A-150 plastic and PAG dosimeters as substitutes for brain tissue in comparison with standard phantom materials such as water and poly(methyl methacrylate). Their findings indicated that the PAG dosimeter presents good simulation of radiation transport in the brain, with discrepancies from the real brain of 10.8%, 5.1%, and 9.4% at a depth of 50 mm for gamma dose, epithermal neutron, and thermal neutron fluence dose distributions, respectively. Finally, they reported that the PAG dosimeter can be considered as a promising substitute for brain tissue, and that it can, as a dosimeter, provide a 3D map of the dose distribution delivered by the epithermal neutron beam (Wojnecki and Green, 2001). Uusi-Simola et al. studied the relative dose response of a BANG-3 gel dosimeter in epithermal neutron irradiation. The elemental composition and density of the BANG-3 gel dosimeter closely matches those of International Commission on Radiation Units and Measurements (ICRU) 44 brain tissue. In epithermal neutron irradiation, the response (R_2) of the gel dosimeter was linearly proportional to the total absorbed dose calculated by the DORT code in ICRU adult brain tissue. This data revealed that the BANG-3 gel dosimeter can be a suitable tool to verify the relative dose distribution of epithermal neutron beams regardless of the LET-dependent response of the gel dosimeter. Moreover, they stated that the presence of neutron-absorbing boron inside Pyrex glass causes it to be less suitable in neutron beams as a container material. Finally, the results revealed the potential of the BANG-3 gel dosimeter in the dosimetry of epithermal neutron beams (Uusi-Simola et al., 2003). Bavarnegin et al. investigated the ability of a NIPAM gel dosimeter to provide the dose distribution resulting from BNCT. In this study, a head phantom filled with the gel was irradiated with the BNCT beam line. The findings demonstrated that the NIPAM gel dosimeter as a lower-toxicity and tissue-equivalent gel dosimeter is an appropriate tool for determining the 3D dose distribution resulting from BNCT. Furthermore, they stated that this gel dosimeter can be a reliable tool in comparison with conventional BNCT dosimetric methods and can be a useful tool in dosimetric verification of BNCT planning because of its abilities to record the 3D dose distribution with high spatial resolution (Bavarnegin et al., 2017). Khajeali et al. measured the dose distribution resulting from BNCT of shallow brain tumors with a NIPAM gel dosimeter. For this purpose, two poly(methyl methacrylate) cylinder phantoms were applied to irradiate the gel dosimeters in front of the BNCT beam. One of the phantoms was filled with only NIPAM gel and the other one included about 20 ml of NIPAM gel with 30 ppm of ^{10}B embedded in the gel dosimeter at a depth of 1 cm from the phantom wall. The results showed an 18% increased dose in the region containing ^{10}B compared with the pure NIPAM gel. Finally, they concluded that the NIPAM gel dosimeter can be used in dosimetric verification of BNCT planning (Khajeali et al., 2017).

4. Discussion

The irradiation techniques used in radiotherapy need reliable and proper dosimetry, acceptable precision, high-resolution measurements of 3D dose distribution, and verification of the TPS and TPS-generated plans for irradiation of tumors (Kozicki et al., 2017). As stated by Podgorsak, gel dosimetry systems are accurate 3D dosimeters (Podgorsak, 2005). A spider plot as presented by Oldham et al. (2003) is an excellent form for comparison of gel dosimetry systems with conventional dosimetry systems (Fig. 2).

This graphical presentation shows the relative performance of different dosimetry systems such as film, ionization chambers, thermoluminescent dosimeters, and gel dosimeters by considering the parameters of volume measured, cost, accuracy, spatial resolution, three-dimensionality, time required for the measurement, and energy dependence. Compared with other detectors, gel dosimeters are favorable

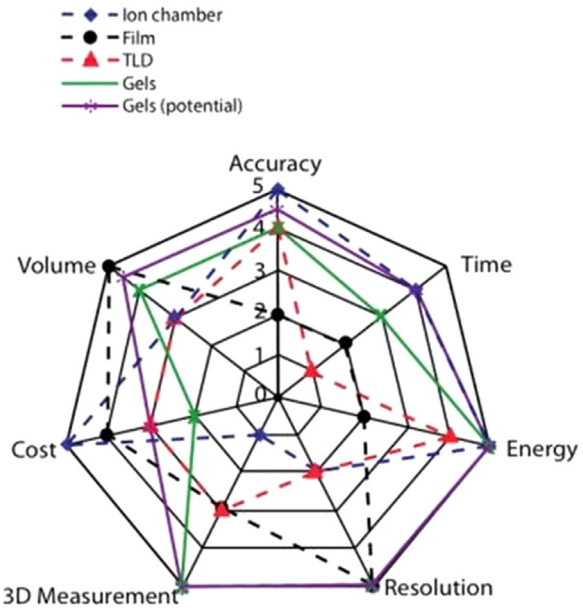

Fig. 2. Spider plot presented by Oldham et al. (2003) comparing several common dosimetry systems. TLD, thermoluminescent dosimeter. Reproduced with permission from Oldham.

in most properties, including their volumetric nature, relative accuracy, high resolution, inherent three-dimensionality, and beam energy independency over much of the significant beam energy range.

Some studies have been conducted recently in the fields of development and optimization of gel compositions (toxicity, melting point, gelling agents other than gelatin, etc.) (Senden et al., 2006; Fong et al., 2001; Fernandes et al., 2008; Pavoni and Baffa, 2012; Hill et al., 2002; Abtahi and Abandansari, 2017), readout systems of gel dosimeters (Cheng et al., 2011; Papadakis et al., 2010; Watanabe and Kubo, 2011; Wuu and Xu, 2011), dosimetric characteristic improvements (Sedaghat et al., 2011a, 2011b; Chiang et al., 2013; Vandecasteele et al., 2011), and investigation of the response of polymer gel dosimeters to different beams (gamma, proton, carbon, electron, and neutron beams) (Wuu et al., 2002; Trapp et al., 2004; Gopishankar et al., 2012; Moutsatsos et al., 2009; Novotný et al., 2002; Gustavsson et al., 2004; Zeidan et al., 2010; Da Silveira et al., 2011; Pianoschi et al., 2010; Bartesaghi et al., 2009; Gambarini et al., 2010; Uusi-Simola et al., 2007).

For clinical applications, it is necessary to investigate the accuracy, dose resolution, reproducibility, and sensitivity of polymer gel dosimeters and also their response to beam energy, dose rate, etc. In the following sections, some dosimetric and structural characteristics of the polymer gels are presented. In addition, the properties of different polymer gel dosimeters used in clinical applications in radiotherapy are discussed.

4.1. Accuracy

Both spatial and dosimetric accuracy of polymer gel dosimeters must be considered in the final response of a gel dosimetry experiment. When the spatial dose distribution is measured, theoretically it is impossible to distinguish spatial and dosimetric errors from each other (Baldock et al., 2010). The gamma index defined by Low et al. (1998) can be used to encompass both the spatial and the dosimetric performance of gel dosimeters in one parameter. Different sources can result in loss of accuracy, as explained in detail by Baldock et al. (2010)

By evaluating the studies listed in Table 1, we found that most polymer gel dosimeters have sufficient accuracy, considering different acceptance criteria in various studies. As stated by Baldock et al. (2010) the basic problem in assessment of the final accuracy of the dose maps provided by gel dosimeters is that there is no gold standard for comparison of the 3D dose distribution. For evaluation of the accuracy of gel dosimeters, the doses obtained with them are mostly compared with doses obtained with the most reliable dosimeters, which use a certain spatial dimension. For example, in 1D, percentage depth dose or dose profiles obtained with gel dosimeters can be compared with those obtained with a diamond detector or an ionization chamber (De Deene et al., 1998; Haraldsson et al., 2000). In 2D, film dosimetry is a suitable tool for evaluating the accuracy of gel dosimeters (De Deene et al., 2000; Pappas et al., 2001). In 3D, most comparisons have been performed with a TPS (Ibbott et al., 1997; Grebe et al., 2001; Ramm et al., 2000), as the treatment plan verification is the most important application of gel dosimeters in quality assurance of radiotherapy so far.

The factors affecting the accuracy can be categorized in two groups: (a) dosimetric factors such as chemical stability, spatial stability, energy-dependent response, dose rate–dependent response, temperature dependency, tissue equivalency, recipient wall effects, voxel shape imaging artifacts, etc. that can lead to deviations between the prescribed dose and the measured dose; and (b) spatial deviations such as phantom positioning error, volumetric contraction of the gel dosimeter, and imaging artifacts that can cause discrepancies in the spatial distribution of the delivered dose (Baldock et al., 2010).

4.2. Dose resolution

The concept of dose resolution introduced by Baldock et al. (2001) is used to estimate the intrinsic dosimetric precision in terms of scanning signal-to-noise ratio and dose sensitivity. The minimal separation of two detectable absorbed doses with a certain level of confidence, *p*, is called *dose resolution*. This is dependent on both the signal acquisition system and the dosimeter itself, and is independent of stochastic variations in dose delivery, chemical concentrations, or the calibration procedure. It is notable that the dose resolution can be used as the criterion to compare and optimize various types of gel dosimeters for a certain set of scanning parameters. In conclusion, the concept of dose resolution is very practical in helping the optimization of the MRI sequence, as the findings may differ if various scanning parameters are applied.

Hilts et al. evaluated the response of a PAG dosimeter using x-ray CT. Their results showed that the dose resolution of the PAG dosimeter is about 50 cGy for an image thickness of 1 cm. Therefore, they reported that despite the low dose resolution, the X-ray CT technique provides accurate localization of high dose gradients such as those seen in stereotactic radiosurgery (Hilts et al., 2000). Trapp et al. investigated the dose response of acrylamide-based gel dosimeters with different compositions using X-ray CT. They reported that the minimum dose resolution is about 1 Gy for low doses, as the dose resolution deteriorates at higher doses, especially in the several gray doses. Furthermore, their findings showed that the dose resolution is optimal for gel dosimeters with 3% acrylamide, 3% *N*,*N*′-methylenebisacrylamide (Bis), 5% gelatin, and 89% water (Trapp et al., 2001). Hurley et al. investigated the dose response of a MAGIC gel dosimeter around point-source irradiation from a brachytherapy source. They reported that the dose resolution of this gel dosimeter is lower than 0.5 Gy for the 0–10 Gy dose range (Hurley et al., 2006). Crescenti et al. changed the relative amount of the components of the MAGIC gel dosimeter to provide linear and steep dose-response relationships. Their findings revealed a mean dose resolution of less than 0.13 Gy for IMRT and a dose resolution from 0.97 to 2.15 Gy for radiosurgery in 5 and 40 Gy doses, respectively (Crescenti et al., 2007). Cho et al. assessed the dose response of a normoxic poly(methacrylic acid) gel dosimeter using optimal CT. They reported that the relative dose resolution (at the 95% confidence level) is 18.4%, which is higher than that of PAG dosimeters (between 4.8% and 17.5% depending on the composition). Moreover, they mentioned that MAGAT and PAGAT gel dosimeters have relative dose resolutions of 7.9% and 11.8–14.6%, respectively (Cho et al., 2012). Khadem-Abolfazli et al. investigated the dose response of a MAGIC-A gel dosimeter. Their findings showed that the dose resolution for doses less than 5 Gy is less than 0.7 Gy and for higher doses increases to 1 Gy (Khadem-Abolfazli et al., 2013). Silveira et al. measured the dose resolution of a MAGIC-f gel dosimeter and reported that it is 0.2 Gy (at the 95% confidence level) (Silveira et al., 2017). Jirasek et al. proposed a 2-propanol-based gel dosimeter formulation (NIPAM monomer) with a high %T (T expresses the total mass fraction of monomers used in the recipe) for x-ray CT gel dosimetry. Their results showed that 16%T gel dosimeters imaged with X-ray CT have lower dose resolutions than previous formulations. At the 67% confidence level and for the 16%T gel dosimeter, the dose resolution was in the 0.2–0.3 Gy range over a 0–30 Gy dose range (i.e., dose resolution less than 0.9 Gy at the 95% confidence level). Also, they reported that the dose resolution in unfiltered images is about 0.1 Gy higher than in filtered images (Jirasek et al., 2010). Kipouros et al. assessed the dynamic dose range and the linear dose response of a VIPAR-based gel dosimeter. Their findings demonstrated that the VIPAR gel dosimeter has a dose resolution of 2% at a dose of 25 Gy. Furthermore, they stated a PAG dosimeter has lower dose resolution, as it usually shows greater dose sensitivity in comparison with a VIPAR gel dosimeter. Also, they mentioned that averaging and/or smoothing gel dosimeter data can lead to improvement of dose resolution (Kipouros et al., 2001). Kozicki et al. evaluated the dose response of an improved VIPAR gel dosimeter. The dose resolution of this gel dosimeter in the whole linear dose range was from 0.65 to 1.35 Gy. Furthermore, they reported that the dose resolution obtained in their study is lower than that of a high %T NIPAM gel dosimeter and

also that it seems to be comparable with that of a 50%C (C expresses the mass fraction of the monomers used in the recipe that is crosslinker), 6%T NIPAM gel dosimeter for the 10–30 Gy dose range (Kozicki et al., 2017). Abtahi and Abandansari investigated the properties of a polymer gel dosimeter with cross-linked poly(vinyl alcohol) as a gelatinous matrix. Their findings demonstrated that the dose resolution increases with increasing absorbed dose. Furthermore, the minimum and maximum dose resolution (at the 95% confidence level) for this gel dosimeter were 0.085 and 0.190 Gy, respectively, which were related to the lowest (30 Gy) and highest (45 Gy) absorbed dose in the dynamic range evaluated (Abtahi and Abandansari, 2017).

4.3. Sensitivity

For a polymer gel dosimeter, the sensitivity is defined as the slope of the linear part of the dose response, which is named the *response-dose sensitivity* (De Deene et al., 2006). Similarly to the dose resolution, sensitivity is a useful quantity to compare various gel formulations and MRI techniques. This quantity affects the minimum detectable dose, dose resolution, and calibration error estimation (Abtahi et al., 2014; Baldock et al., 2001; De Deene, 2004).

Baldock et al. reported that the mean sensitivity of a PAG dosimeter in the range up to 10 Gy is 0.03 Gy^{-1} s^{-1} (Baldock et al., 1998). It is notable that different concentrations of both gelatin and acrylamide and Bis lead to differences in sensitivity (Baldock et al., 1996a; Maryanski et al., 1997; Audet et al., 1996). Lepage et al. found that depending on the monomers used in the PAG formulation, the dose sensitivities change in the range from 0.33 to 1.19 Gy^{-1} s^{-1} (Lepage et al., 2001). Pourfallah et al. showed that for dose ranges of 0–20 Gy and 20–40 Gy, the R_2 dose sensitivity of PAGAT gel is 0.09 and 0.08 Gy^{-1} s^{-1}, respectively (Pourfallah et al., 2012). A chief deficiency of acrylamide-based gel dosimeters is their relatively low sensitivity. In this regard, several researchers increased the sensitivity of the acrylamide-based polymer gels. Abtahi et al. increased the sensitivity of a PAGAT gel dosimeter by adding urea and glucose, and the new formulation was called *PAGATUG*. They reported that the R_2 sensitivity of the PAGATUG gel dosimeter in comparison with a PAGAT gel dosimeter was increased by a factor of about 2.6 (0.509 Gy^{-1} s^{-1} vs. 0.192 Gy^{-1} s^{-1}) (Abtahi et al., 2014). Yoshioka et al. reported that the dose sensitivity of a polyacrylamide-based gel dosimeter was increased by addition of sucrose (Yoshioka et al., 2010). Fong et al. indicated that the dose sensitivities of a MAGIC gel dosimeter in the 0–30 Gy range at 20 MHz are 0.68, 0.52, and 0.30 Gy^{-1} s^{-1}, respectively, when the concentration of methacrylic acid is 3%, 6%, and 9%, respectively. Furthermore, they showed that the dose sensitivities increased to 0.87, 0.57, and 0.31 Gy^{-1} s^{-1} at 85 MHz (Fong et al., 2001). Hurley et al. evaluated the response of a MAGAT gel dosimeter using MRI. The R_2 dose sensitivity obtained for this gel dosimeter ranged from 1.65 to 8.18 Gy^{-1} s^{-1} for the different concentrations of methacrylic acid and gelatin used in the MAGAT gel formulation (Hurley et al., 2005). Venning et al. presented the R_2 dose response of a methacrylic acid, gelatin, and ascorbic acid (MAGAS) gel dosimeter for doses up to 25 Gy. Their results showed an R_2 dose sensitivity of 0.50 Gy^{-1} s^{-1} (Venning et al., 2005a). Fernandes et al. added 3% formaldehyde to a MAGIC gel dosimeter formulation (MAGIC-f). The formaldehyde increased the sensitivity of the MAGIC-f gel dosimeter by about 10% (1.05 Gy^{-1} s^{-1} vs. 0.95 Gy^{-1} s^{-1}) (Fernandes et al., 2008). Pavoni and Baffa added 3.3% formaldehyde to a MAGIC gel formulation and showed increased thermal stability of the gel dosimeter prepared. Their MAGIC-f gel dosimeter irradiated with ^{60}Co beams and 10 MV beams had dose sensitivities of 0.67 and 0.63 Gy^{-1} s^{-1}, respectively (Pavoni and Baffa, 2012). Hayashi et al. evaluated the effect of inorganic salt on the dose sensitivity of a methacrylic acid–based gel dosimeter. They found that the dose sensitivity of the methacrylic acid–based gel dosimeter was enhanced by the addition of inorganic salts. They reported that the slopes of the R_2 dose response curves for the samples with 0.0, 0.5, and 1.0 M $MgCl_2$ were 3.14, 5.56, and 8.93 Gy^{-1} s^{-1}, respectively (Hayashi et al., 2010). Abtahi et al. added agarose to the MAGIC gel formulation (MAGIC-A). They indicated that the dose sensitivity of the MAGIC-A gel dosimeter for gamma irradiation is 0.38 Gy^{-1} s^{-1}, which decreased to 0.18 Gy^{-1} s^{-1} for thermal neutron irradiation (Abtahi et al., 2016). Pantelis et al. reported a poly(ethylene glycol) diacrylate, Bis, and gelatin (PABIG) gel dosimeter with a dose sensitivity of 0.11 and 0.14 Gy^{-1} s^{-1} at 11 and 26 days after irradiation, respectively (Pantelis et al., 2006). Pappas et al. irradiated VIPAR gel dosimeters in the dose range from 0 to 12 Gy and then scanned them by MRI. The dose sensitivity was 0.10 Gy^{-1} s^{-1} for this gel dosimeter. Furthermore, they indicated that this dose sensitivity does not change with time and is not reduced even when a boost dose of 2.5 Gy is used 15 days after the first irradiation (Pappas et al., 1999). Kozicki et al. improved the VIPAR gel dosimeter by altering the concentrations of the *N*-vinylpyrrolidone and Bis monomeric components in co-solvent solutions. They reported a maximum dose sensitivity of 0.17 Gy^{-1} s^{-1} for the new gel dosimeter by NMR measurements (Kozicki et al., 2017). Maryanski et al. reported a linear dose response up to about 8 Gy for a BANG gel dosimeter, with a dose sensitivity of 0.25 Gy^{-1} s^{-1} obtained by MRI (Maryanski et al., 1994). Oldham et al. increased the comonomer concentration of a BANG gel dosimeter (100% higher than in the dosimeter developed by Maryanski et al. (1994), and concluded that the dose sensitivity increased to 70% (Oldham et al., 1998). Koeva et al. reported the dose sensitivities of NIPAM gel dosimeters for different recipes. For example, for a recipe of 6%T, %50 C, and without a co-solvent, the dose sensitivity of the NIPAM gel dosimeter was 0.07 Gy^{-1} s^{-1}, and for a recipe of 10%T, 50%C, and with a co-solvent (2-propanol), it was 0.15 Gy^{-1} s^{-1}. Increasing the solubility of Bis in NIPAM-based gel dosimeters by addition of a co-solvent such as 2-propanol and glycerol leads to an increase of dose sensitivity (Koeva et al., 2009). Chen et al. reported that in the 0–12 Gy dose range, the dose sensitivity of a NIPAM gel dosimeter was 0.11 Gy^{-1} s^{-1} (Chen et al., 2014). Hsieh et al. measured the dose distribution for fixed and moving irradiation targets. Their findings showed that the mean dose sensitivities of fixed and moving NIPAM gel dosimeters are 0.136 and 0.137 Gy^{-1} s^{-1}, respectively (Hsieh et al., 2015). Farhood et al. (2018a) reported that in the 0–10 Gy dose range, the dose sensitivity of a poly(2-acrylamido-2-methylpropane sulfonic acid sodium salt) and gelatin (PASSAG) gel dosimeter is between 0.13 and 0.15 Gy^{-1} s^{-1}. To directly compare the dose sensitivities of various polymer gel dosimeters with each another, the aforementioned data are summarized in Table 2.

Several studies reported the dose sensitivity of polymer gel dosimeters by using X-ray CT (Hilts et al., 2000; Kozicki et al., 2017; Brindha et al., 2004; Hill et al., 2005; Sellakumar et al., 2010; Shih et al., 2017).

4.4. Reproducibility

An important factor that can influence the results obtained from a dosimetric system is the reproducibility of the dose response. The reproducibility of polymer gel dosimeters is classified in two groups: intrabatch reproducibility and interbatch reproducibility.

De Deene reported the intrabatch and interbatch reproducibility of PAG dosimeters is equivalent to 0.9% and 0.08% of the total dose range, respectively (De Deene, 2004). Cosgrove et al. investigated the reproducibility of a PAG dosimeter and reported that response of this dosimeter for the more than 50% isodose curves is very reproducible, as the standard deviation on all the regions around the 50–90% isodose curves was 6.4%. However, for the lower isodose curves, the variance was larger (Cosgrove et al., 2000). Bayreder et al. investigated the dose reproducibility of MAGAT for different tetrakis(hydroxymethyl)phosphonium chloride concentrations. Their results demonstrated that the dose reproducibility for voxel volumes of approximately $1.4 \times 1.4 \times 2\,mm^3$ was better than 2% (Bayreder et al., 2006). Cho et al. evaluated the dosimetric properties of normoxic poly(methacrylic

Table 2
The dose sensitivity of various polymer gel dosimeters.

Gel type	Linear dose range (Gy)	Dose sensitivity (Gy^{-1} s^{-1})	Reference
PAG	0–10	0.03	Baldock et al. (1998)
PAGAT	0–20 and 20–40	0.09 and 0.08	Pourfallah et al. (2012)
PAGATUG	1.5–3.5	0.51	Abtahi et al. (2014)
MAGIC	0–30	0.30–0.87	Fong et al. (2001)
MAGAT	–	1.65–8.18	Hurley et al. (2005)
MAGAS	0–25	0.50	Venning et al. (2005a)
MAGIC-f	0–10	1.05	Fernandes et al. (2008)
MAGIC-A	1–12.5	0.38	Abtahi et al. (2016)
PABIG	0–15	0.11	Pantelis et al. (2006)
VIPAR	0–12	0.10	Pappas et al. (1999)
BANG	0–8	0.25	Maryanski et al. (1994)
NIPAM	0–21	0.07–0.15	Koeva et al. (2009)
PASSAG	0–10	0.13–0.15	Farhood et al. (2018a)

MAGAS, methacrylic acid, gelatin, and ascorbic acid; MAGAT, methacrylic acid, gelatin, and tetrakis(hydroxymethyl)phosphonium chloride; MAGIC, methacrylic acid, ascorbic acid, gelatin, and copper; MAGIC-A, methacrylic acid, ascorbic acid, gelatin, copper, and agarose; MAGIC-f, methacrylic acid, ascorbic acid, gelatin, copper, and formaldehyde; NIPAM, *N*-isopropylacrylamide; PABIG, poly(ethylene glycol) diacrylate, *N*,*N* ′-methylenebisacrylamide, and gelatin; PAG, polyacrylamide gel; PAGAT, polyacrylamide, gelatin, and tetrakis (hydroxymethyl)phosphonium chloride; PAGATUG, polyacrylamide, gelatin, and tetrakis(hydroxymethyl)phosphonium chloride, urea, and glucose; PASSAG, poly (2-acrylamido-2-methylpropane sulfonic acid sodium salt) and gelatin; VIPAR, *N*-vinylpyrrolidone-argon.

acid) gel dosimeters using optimal CT. They reported that the reproducibility of the gel dosimeters irradiated with 2 and 4 Gy was 2.0% and 2.1%, respectively (Cho et al., 2012). Maryanski et al. (1994) reported that the variation of the R_2 dose response of a BANG gel dosimeter is reproducible and is less than 2%. Farajollahi et al. evaluated the properties of a BANG gel dosimeter in low-dose-rate brachytherapy. Their findings showed that the dose-response curves are reproducible over the measured dose range (0–10 Gy), as they reported an intrabatch reproducibility of within ± 4% for the BANG gel dosimeter (Farajollahi et al., 1999). Venning et al. reported an interbatch reproducibility of up to 5% difference in the dose for a MAGAS gel dosimeter (Venning et al., 2005a). Farajollahi et al. indicated that the dose response of a NIPAM gel dosimeter is reproducible in the same and various batches of chemical. They reported that the intrabatch reproducibility and interbatch reproducibility of NIPAM gel are 3% and 2%, respectively (Farajollahi et al., 2014). Ghaseminejad et al. evaluated the reproducibility of the absorbed dose response of a NIPAM gel dosimeter. Their findings showed that the dose response is highly reproducible over the measured dose range (0–12 Gy) and is within ± 3% (Ghaseminejad et al., 2017).

4.5. Effect of dose rate

An ideal dosimeter must be able to measure the 3D dose distribution with a constant response irrespective of the dose rate. Given that the dose rate is spatially dependent, it is necessary for any gel dosimeter that its response be relatively insensitive to the dose rate. The dose rate–dependent response of polymer gel dosimeters is dependent on the type of polymer gel.

Several studies have investigated the effect of the dose rate dependency of different polymer gel dosimetry systems. Novotny et al. evaluated the dependence of a BANG-2 gel dosimeter on dose rates of 80, 160, 240, 320, and 400 Monitor unit (MU)–min^{-1}. The results showed that there is no trend in the dependence of the BANG-2 gel dosimeter dose sensitivity on the dose rate for both electron beams and photon beams (Novotny et al., 2001). Senden et al. evaluated the dose rate dependency response of various polymer gel dosimeters (NIPAM/Bis, diacetone acrylamide [DAAM]/Bis, PAGAT, and *N*-vinylformamide [NVF]/Bis) at dose rates of 55 and 272 cGy min^{-1}. They showed that the dose rate does not remarkably affect the response of the polymer gels irradiated with 15 and 50 Gy. Furthermore, their findings revealed the NIPAM/Bis gel dosimeter has lower dependency on the dose rate than the PAGAT gel dosimeter (Senden et al., 2006). Bayreder et al. investigated the dose rate dependency of a MAGAT gel dosimeter in low-, medium-, and saturation-dose regions. They showed that the presence of tetrakis(hydroxymethyl)phosphonium chloride in MAGAT, as an oxygen scavenger, results in high sensitivity to the dose but that the dose response firmly depends on the dose rate in the high- and medium-dose regions. Furthermore, only at low doses (2 Gy) was a dose rate dependence not found. So, they concluded that in dosimetry with MAGAT gel, tetrakis(hydroxymethyl)phosphonium chloride should be used only in the low-dose region away from saturation (Bayreder et al., 2006). In studies by Adinehvand et al. and Azadbakht et al., the effects of dose rates of 80, 160, 240, 320, 400, and 480 cGy min^{-1} on the response of MAGIC-A and PAGAT gel dosimeters in electron beams were investigated. The data showed that there is no trend in the R_2 dependency on the mean dose rate (Adinehvand et al., 2008; Azadbakht et al., 2009). Zehtabian et al. evaluated the dose rate–dependent response of a PAGAT gel dosimeter at low dose rates. Their results showed that the response of the PAGAT gel dosimeter would be affected by oxygen. They reported that oxygen diffusion through plastic vials would affect the response of a gel dosimeter for dose rates lower than 2 Gy h^{-1}. Therefore, they recommended that glass vials be used instead of plastic vials for dosimetry purposes for low-dose-rate sources. However, when plastic vials or phantoms are used for such sources they should be kept in oxygen-free conditions. Furthermore, their findings showed that the use of plastic vials does not have a considerable effect on the PAGAT gel dosimeter response for dose rates of 2 Gy h^{-1} or more (Zehtabian et al., 2012). Farajollahi et al. investigated the dependency of the response of a NIPAM gel dosimeter on the dose rate. Their findings showed that the response of the NIPAM gel dosimeter is not affected by the dose rate (Farajollahi et al., 2014). Waldenberg et al. characterized the dose rate dependency of a NIPAM gel dosimeter for dose rates of 100, 300, and 600 MU min^{-1}. They found that the dose response of the NIPAM gel dosimeter is dependent on the dose rate (Waldenberg et al., 2017). Farhood et al. evaluated the dependency of the response of a PASSAG gel dosimeter on dose rates of 100, 200, 300, and 400 cGy min^{-1}, and reported that the R_2 dose response and sensitivity of this gel dosimeter are not affected by the dose rate (Farhood et al., 2018a).

4.6. Effect of beam energy

One of the physical factors that can affect the gel dosimeter response is the beam energy, and this needs to be investigated individually.

Maryanski et al. reported that a BANG-2 gel dosimeter has a linear dose response with beam energy independency for a range of photon and electron beams (Maryanski et al., 1996a, 1996b). In studies by Farajollahi et al. and Baldock et al., BANG gel dosimeters were irradiated with photon energies of 300 kV, 660 keV, 1.25 MeV, 6 MV, 8 MV, and 16 MV and electron energies of 5, 7, 9, 12, 15, 17, and 20 MeV. They concluded that the dose response of the BANG gel dosimeter is independent of electron and photon energies (Farajollahi et al., 1999; Baldock et al., 1996b). Novotny et al. investigated the dependency of BANG-2 gel dosimeter sensitivity on X-ray photon energies of 4, 6, and 18 MV and electron energies of 9, 12, 16, and 20 MeV. Their results demonstrated a trend in the dependence of the gel dosimeter sensitivity on X-ray photon and electron energies, as the gel dosimeter sensitivity has a decreasing trend with increasing electron or photon energy (Novotny et al., 2001). Pantelis et al. and Venning et al. evaluated the beam energy dependence of several normoxic polymer gel dosimeters.

The gel dosimeters used in these studies were BANG-1, BANG-2, BANG-3, VIPAR, PABIG, MAGIC, MAGAS, and MAGAT gel dosimeters. They reported that the dose response of these normoxic polymer gel dosimeters is independent of beam energy over the wide range from 100 keV to 10 MeV (Pantelis et al., 2004; Venning et al., 2005b). De Deene et al. assessed the dose response of a normoxic methacrylic acid–based gel (nMAG) dosimeter and acrylamide-based gel (PAG and normoxic PAG [nPAG]) dosimeters for photon energies of 6 and 25 MV. They concluded that there is no change in the dose response of the PAG and nPAG dosimeters, but a small change was found with increasing photon energy for the nMAG dosimeter (De Deene et al., 2001, 2006). Adinehvand et al. investigated the dependency of the response of a MAGIC-A gel dosimeter on electron energies of 4, 6, 12, and 18 MeV. They found that the sensitivity of the MAGIC-A gel dosimeter is dependent on the electron energy, as the gel dosimeter response increased with increasing electron energy (Adinehvand et al., 2008). Sathiyaraj et al. evaluated the energy dependency of a MAGAT gel dosimeter on photon energies of 6 and 10 MV. Their finding showed that the energy dependency of the MAGAT gel dosimeter is not significant (Sathiyaraj and Samuel, 2018). Sellakumar et al. assessed the beam energy dependency of a PAGAT gel dosimeter on photon energies of 1.25 MeV, 6 MV, and 15 MV and electron energies of 6, 9, 12, 15, 18, and 21 MeV. They reported that the dependence of the PAGAT gel dosimeter sensitivity on various electron and photon energies is insignificant (Sellakumar et al., 2010). Farajollahi et al. investigated the dose response of a NIPAM gel dosimeter on photon energies of 9 MV and 1.25 MeV. Their results revealed that the dose response of the NIPAM gel dosimeter is not dependent on beam energy (Farajollahi et al., 2014). Shih et al. assessed the dose response of an n-NIPAM gel dosimeter on electron energies of 6, 9, and 12 MeV. Their data showed that the energy dependency of this gel dosimeter is negligible as the sensitivity variation for different electron energies was less than 2% (Shih et al., 2017). Farhood et al. (2018a) evaluated the dependency of the response of a PASSAG gel dosimeter on photon energies of 6 and 18 MV and reported that the R_2 dose response and sensitivity of this gel dosimeter are not affected by photon energy.

4.7. Toxicity

One of the main limitations of polymer gel dosimeters for use in routine clinical applications is the problem of toxicity of monomers (Waldenberg et al., 2017).

The use of noxious monomers such as acrylamide and Bis is a concern among researchers. Therefore, acrylamide-based gel dosimeters such as PAG, PAGAT, and similar gels must be prepared, used, and disposed of with great care. Acrylamide is a serious neurotoxin and a suspected human teratogen and carcinogen that is easily absorbed via the skin. The oral median lethal dose (LD_{50}) of acrylamide is approximately 124 mg kg^{-1} in rats (Sigma-Aldrich, 2013a). In this regard, several researchers have attempted to discover new monomers with lower toxicity.

Senden et al. replaced very toxic acrylamide with less harmful DAAM, NVF, and NIPAM. Their results showed that the dose response of a NIPAM gel dosimeter is comparable to that of a PAGAT dosimeter in terms of low dependency on the dose rate and irradiation temperature and high dose sensitivity. In addition, the dose response of NIPAM revealed a linear trend over a higher dose range than that of PAGAT. Two other gel dosimeters (DAAM and NVF gel dosimeters) had remarkably lower dose sensitivities (Senden et al., 2006). It is noteworthy that the NIPAM gel dosimeter has an oral LD_{50} of 375 mg kg^{-1}, and so NIPAM is still a toxic monomer (Sigma-Aldrich, 2013b). However, NIPAM is very expensive, which increases the total cost of gel dosimeter production. Pappas et al. introduced a VIPAR gel dosimeter. This gel dosimeter contains *N*-vinylpyrrolidone, which has an oral LD_{50} of 1022 mg kg^{-1} (Pappas et al., 1999). However, *N*-vinylpyrrolidone is suspected of having carcinogenic effects (BASF, 2015). Abtahi introduced a new polymer gel dosimeter (PAMPSGAT gel dosimeter). In this gel dosimeter, the polyacrylamide monomer, which is extremely toxic, is replaced by the monomer 2-acrylamido-2-methylpropane sulfonic acid (Abtahi, 2016), which is less toxic, with an oral LD_{50} of 1838 mg kg^{-1}, and also cost-effective (Sigma-Aldrich, 2014). This monomer showed remarkably lower toxicity compared with acrylamide, NIPAM, and *N*-vinylpyrrolidone. On the other hand, the use of hydroquinone, with an oral LD_{50} of 320 mg kg^{-1}, as a free-radical scavenger in polymer gel dosimeters is considered another toxic source, and this substance has been not used in PAMPSGAT gel dosimeters (Abtahi, 2016). Moreover, 2-acrylamido-2-methylpropane sulfonic acid has shown a negative response in carcinogenicity tests (Sigma-Aldrich, 2014). Farhood et al. recently developed a new polymer gel dosimeter with negligible toxicity. In this study, 2-acrylamido-2-methylpropane sulfonic acid sodium salt was used instead of acrylamide in a PAGAT gel dosimeter, and the new formulation was called *PASSAG*; that is, poly(2-acrylamido-2-methylpropane sulfonic acid sodium salt) and gelatin. The monomer used in the PASSAG gel dosimeter is a safe substance with $LD_{50} > 16{,}000$ mg kg^{-1} and negative genetic toxicity and carcinogenicity test results and is eco-friendly (Farhood et al., 2018b).

4.8. Melting point

Increasing the melting point of the polymer gel dosimeters is necessary for their use in higher-temperature conditions, such as a reactor thermal column, or to allow convenient gel preparation in practical environments. In addition to radiotherapy modalities with gamma radiation, the improved gel dosimeters can be used for dosimetric purposes in treatment modalities with thermal/epithermal neutrons such as BNCT.

Recently, several researchers recommended substances for increasing the melting point (Fernandes et al., 2008; Pavoni and Baffa, 2012). Pavoni et al. used formaldehyde to increase the melting point of a MAGIC gel dosimeter (Fernandes et al., 2008; Pavoni and Baffa, 2012). One shortcoming of conventional methacrylic acid–based gel dosimeters such as MAGIC gel dosimeter is their low melting point. MAGIC gel dosimeters have a melting point of about 25 °C, which is not suitable for use in higher-temperature conditions. They reported that formaldehyde added to MAGIC gel (MAGIC-f) increases its melting point from 25 to 69 °C (Fernandes et al., 2008; Pavoni and Baffa, 2012). However, formaldehyde is very toxic and the toxicity of the MAGIC-f polymer gel is greater than that of the MAGIC polymer gel. Abtahi et al. added agarose to the MAGIC gel formulation to increase its melting point (agarose is nontoxic). Addition of agarose increased the melting point to 60 °C without adding any extra toxicity (Abtahi et al., 2016).

5. Conclusion

The propose of gel dosimetry in clinical applications is to obtain an integrated 3D dose distribution in anthropomorphic phantoms. In this regard, different polymer gel dosimeters have been used by researchers. In the current work, most gel dosimeters studied showed acceptable dose accuracy as a 3D dosimeter with high resolution.

Among the important features of polymer gel dosimeters for clinical applications are the accuracy, dose resolution, reproducibility, and sensitivity and also the dependence of their response to beam energy, dose rate, etc. Acrylamide-based gel dosimeters are highly toxic, and their sensitivity and dose resolution are relatively low and high, respectively. However, their dose response is not affected by dose rate and beam energy. Methacrylic acid–based gel dosimeters have high dose sensitivity and lower toxicity, while their dose response is beam energy dependent. NIPAM gel dosimeters have low dose resolution, but their sensitivity is lower and they are relatively toxic. Therefore, it is difficult to judge which is the best gel dosimeter to use in the clinic because each polymer gel dosimeter has its advantages and limitations.

Researchers are attempting to develop and optimize polymer gel

dosimeters. In this regard, several polymer gel dosimeters have recently been introduced; for example, PASSAG (negligible toxicity), PVA, Bis, Acrylamide and THPC (PVABAT) (lower dose resolution), and MAGIC-A (increased melting point without imposing any additional toxicity) gel dosimeters. However, the other dosimetric characteristics of the new polymer gel dosimeters for use in the clinic should be investigated.

References

Abtahi, S., 2016. Characteristics of a novel polymer gel dosimeter formula for MRI scanning: dosimetry, toxicity and temporal stability of response. Phys. Med. 32, 1156–1161.

Abtahi, S., Aghamiri, S., Khalafi, H., Rahmani, F., 2014. An investigation into the potential applicability of gel dosimeters for dosimetry in boron neutron capture therapy. Int. J. Radiat. Res. 12, 139–149.

Abtahi, S.M., Aghamiri, S.M.R., Khalafi, H., 2014. Optical and MRI investigations of an optimized acrylamide-based polymer gel dosimeter. J. Radioanal. Nucl. Chem. 300, 287–301.

Abtahi, S.M., Zahmatkesh, M.H., Khalafi, H., 2016. Investigation of an improved MAA-based polymer gel for thermal neutron dosimetry. J. Radioanal. Nucl. Chem. 307, 855–868.

Abtahi, S.M.M., Abandansari, H.S., 2017. Polymer gel dosimeters with PVA–GA matrix. Australas. Phys. Eng. Sci. Med. 40, 651–658.

Adinehvand, K., Zahmatkesh, M., Aghamiri, M., Akhlaghpour, S., Bagheri, S., 2008. Verification of dose rate and energy dependence of MAGICA polymer gel dosimeter with electron beams. Iran. J. Radiat. Res. 6, 31–36.

Amin, M.N., Horsfield, M.A., Bonnett, D.E., Dunn, J., Poulton, M., Farding, F., 2003. A comparison of polyacrylamide gels and radiochromic film for source measurements in intravascular brachytherapy. Br. J. Radiol. 76, 824–831.

Audet, C., Duzenli, C., Kwa, W., Tsang, V., Mackay, A., 1996. An example of MRI polymer gel dosimetry applied to 3-D conformal radiotherapy. Med. Phys. 23, 803.

Azadbakht, B., Hadad, K., Zahmatkesh, M., 2009. Response verification of dose rate and time dependence of PAGAT polymer gel dosimeters by photon beams using magnetic resonance imaging. J. Phys. Conf. Ser. 164, 012036.

Baker, C.R., Quine, T.E., Brunt, J.N.H., Kacperek, A., 2009. Monte Carlo simulation and polymer gel dosimetry of 60 MeV clinical proton beams for the treatment of ocular tumours. Appl. Radiat. Isot. 67, 402–405.

Baldock, C., Burford, R., Billingham, N., Cohen, D., Keevil, S., 1996a. Polymer gel composition in magnetic resonance imaging dosimetry. Med. Phys. 23, 1070.

Baldock, C., Greener, A., Billingham, N., Burford, R., Keevil, S., 1996b. Energy response and tissue equivalence of polymer gels for radiation dosimetry by MRI. Proc. Eur. Soc. Magn. Reson. Med. Biol. 2, 312.

Baldock, C., Burford, R., Billingham, N., Wagner, G., Patval, S., Badawi, R., et al., 1998. Experimental procedure for the manufacture and calibration of polyacrylamide gel (PAG) for magnetic resonance imaging (MRI) radiation dosimetry. Phys. Med. Biol. 43, 695.

Baldock, C., Lepage, M., Bäck, S.Å.J., Murry, P., Jayasekera, P., Porter, D., et al., 2001. Dose resolution in radiotherapy polymer gel dosimetry: effect of echo spacing in MRI pulse sequence. Phys. Med. Biol. 46, 449.

Baldock, C., De Deene, Y., Doran, S., et al., 2010. Polymer gel dosimetry. Phys. Med. Biol. 55, 1–63.

Bartesaghi, G., Burian, J., Gambarini, G., Marek, M., Negri, A., Viererbl, L., 2009. Evaluation of all dose components in the LVR-15 reactor epithermal neutron beam using Fricke gel dosimeter layers. Appl. Radiat. Isot. 67, 199–201.

BASF, 2015. N-Vinyl-2-pyrrolidone non-stab. Safety data sheet.

Bavarnegin, E., Khalafi, H., Sadremomtaz, A., Kasesaz, Y., Khajeali, A., 2017. Investigation of dose distribution in mixed neutron-gamma field of boron neutron capture therapy using N-isopropylacrylamide gel. Nucl. Eng. Technol. 49, 189–195.

Bayreder, C., Georg, D., Moser, E., Berg, A., 2006. Basic investigations on the performance of a normoxic polymer gel with tetrakis-hydroxy-methyl-phosphonium chloride as an oxygen scavenger: reproducibility, accuracy, stability, and dose rate dependence. Med. Phys. 33, 2506–2518.

Brindha, S., Venning, A., Hill, B., Baldock, C., 2004. Experimental study of attenuation properties of normoxic polymer gel dosimeters. Phys. Med. Biol. 49, 353.

Cerullo, N., Esposito, J., Daquino, G., 2004. Spectrum shaping assessment of accelerator-based fusion neutron sources to be used in BNCT treatment. Nucl. Instrum. Methods Phys. Res. B 213, 641–645.

Chan M.F., Fung A.Y.C., Hu Y.C., Amols H., Zaider M., Abramson D., 2000. The measurement of three dimensional dose distribution of a ruthenium-106 ophthalmological applicator using magnetic resonance imaging of BANG polymer gels. Paper presented at: World Cong. Med. Phys. Biomed. Eng.

Chen, Y.L., Hsieh, B.T., Chiang, C.M., Shih, C.T., Cheng, K.Y., Hsieh, L.L., 2014. Dose verification of a clinical intensity-modulated radiation therapy eye case by the magnetic resonance imaging of N-isopropylacrylamide gel dosimeters. Radiat. Phys. Chem. 104, 188–191.

Cheng, H.-W., Ho, C.-J., Lee, C.-C., Tu, S.-J., Shih, B.-Y., Chao, T.-C., 2011. Development of a novel optical CT employing a laser to create a collimated line-source with a flat-top intensity distribution. Radiat. Meas. 46, 1932–1935.

Cheng, K.Y., Hsieh, L.L., Shih, C.T., 2016. A comprehensive evaluation of NIPAM polymer gel dosimeters on three orthogonal planes and temporal stability analysis. PLoS One 11, 0155797.

Chiang, C.-M., Hsieh, B.-T., Shieh, J.-I., Cheng, K.-Y., Hsieh, L.-L., 2013. An approach in exploring the fundamental dosimetric characteristics for a long shelf life irradiated acrylamide-based gel. J. Radioanal. Nucl. Chem. 298, 1435–1445.

Cho, K.H., Cho, S.J., Lee, S., Lee, S.H., Min, C.K., Kim, Y.H., et al., 2012. Dose responses in a normoxic polymethacrylic acid gel dosimeter using optimal CT scanning parameters. Nucl. Instrum. Methods Phys. Res. A 675, 112–117.

Cosgrove, V.P., Murphy, P.S., McJury, M., et al., 2000. The reproducibility of polyacrylamide gel dosimetry applied to stereotactic conformal radiotherapy. Phys. Med. Biol. 45, 1195–1210.

Crescenti, R.A., Scheib, S.G., Schneider, U., Gianolini, S., 2007. Introducing gel dosimetry in a clinical environment: customization of polymer gel composition and magnetic resonance imaging parameters used for 3D dose verifications in radiosurgery and intensity modulated radiotherapy. Med. Phys. 34, 1286–1297.

Cuevas, D., Pavoni, J., Baffa, O., 2016. A phantom to study the effects of metallic prostheses in radiotherapy by gel dosimetry. In: MassillonJl, G., Fossion, R., RosadoMendez, I.M., AvilaRodriguez, M.A., LopezPerez, D.A. (Eds.), AIP Conference Proceedings 1747, 060005. The American.

Da Silveira, M.A., Pavoni, J.F., Salmon, C.E.G., Baffa, O., 2014. Tridimensional dosimetry for prostate IMRT treatments using MAGIC-f gel by MRI. Radiat. Meas. 71, 369–373.

Da Silveira, M.C., Sampaio, F.G., Petchevist, P.C., de Oliveira, A.L., de Almeida, A., 2011. Mycosis Fungoides electron beam absorbed dose distribution using Fricke xylenol gel dosimetry. Nucl. Instrum. Methods Phys. Res. B 269, 3137–3140.

De Deene, Y., 2004. Essential characteristics of polymer gel dosimeters. J. Phys. Conf. Ser. 3, 34.

De Deene, Y., De Wagter, C., Van Duyse, B., Derycke, S., De Neve, W., Achten, E., 1998. Three-dimensional dosimetry using polymer gel and magnetic resonance imaging applied to the verification of conformal radiation therapy in head-and-neck cancer. Radiother. Oncol. 48, 283–291.

De Deene, Y., De Wagter, C., Van Duyse, B., Derycke, S., Mersseman, B., De Gersem, W., et al., 2000. Validation of MR-based polymer gel dosimetry as a preclinical three--dimensional verification tool in conformal radiotherapy. Magn. Reson. Med. 43, 116–125.

De Deene, Y., Reynaert, N., De Wagter, C., 2001. On the accuracy of monomer/polymer gel dosimetry in the proximity of a high-dose-rate ^{192}Ir source. Phys. Med. Biol. 46, 2801.

De Deene, Y., Vergote, K., Claeys, C., De Wagter, C., 2006. The fundamental radiation properties of normoxic polymer gel dosimeters: a comparison between a methacrylic acid based gel and acrylamide based gels. Phys. Med. Biol. 51, 653–673.

Deyhimihaghighi, N., Noor, N.M., Soltani, N., Jorfi, R., Haghir, M.E., Adenan, M.Z., et al., 2014. Contrast enhancement of magnetic resonance imaging (MRI) of polymer gel dosimeter by adding platinum nano- particles. J. Phys. Conf. Ser. 546.

Farajollahi, A., Bonnett, D., Ratcliffe, A., Aukett, R., Mills, J., 1999. An investigation into the use of polymer gel dosimetry in low dose rate brachytherapy. Br. J. Radiol. 72, 1085–1092.

Farajollahi, A., Pak, F., Horsfield, M., Myabi, Z., 2014. The basic radiation properties of the N-isopropylacrylamide based polymer gel dosimeter. Int. J. Radiat. Res. 12, 347–354.

Farhood, B., Ghorbani, M., 2015. Effect of diameter of nanoparticles and capture cross-section library on macroscopic dose enhancement in boron neutron capture therapy. J. Contemp. Brachyther. 6, 377–385.

Farhood, B., Geraily, G., Abtahi, S.M., Ghorbani, M., Mehdikhani, M., 2018a. Evaluation of dose rate and photon energy dependence of PASSAG polymer gel dosimeter. J. Radioanal. Nucl. Chem. 317, 1041–1050.

Farhood, B., Abtahi, S.M., Geraily, G., Ghorbani, M., Mahdavi, S.R., Zahmatkesh, M.H., 2018b. Dosimetric characteristics of PASSAG as a new polymer gel dosimeter with negligible toxicity. Radiat. Phys. Chem. 147, 91–100.

Fazli, Z., Sadeghi, M., Zahmatkesh, M.H., Mahdavi, S.R., Tenreiro, C., 2013. Dosimetric comparison between three dimensional treatment planning system, Monte Carlo simulation and gel dosimetry in nasopharynx phantom for high dose rate brachytherapy. J. Cancer Res. Ther. 9, 402–409.

Fernandes, J.P., Pastorello, B.F., de Araujo, D.B., Baffa, O., 2008. Formaldehyde increases MAGIC gel dosimeter melting point and sensitivity. Phys. Med. Biol. 53, 53.

Fong, P.M., Keil, D.C., Does, M.D., Gore, J.C., 2001. Polymer gels for magnetic resonance imaging of radiation dose distributions at normal room atmosphere. Phys. Med. Biol. 46, 3105.

Fuse, H., Shinoda, K., Inohira, M., Kawamura, H., Miyamoto, K., Sakae, T., et al., 2015. Note: utilization of polymer gel as a bolus compensator and a dosimeter in the near-surface buildup region for breast-conserving therapy. Rev. Sci. Instrum. 86, 096103.

Gambarini, G., Agosteo, S., Carrara, M., Gay, S., Mariani, M., Pirola, L., et al., 2006. In-phantom dosimetry for BNCT with Fricke and normoxic-polymer gels. J. Phys. Conf. Ser. 41, 275–281.

Gambarini, G., Bartesaghi, G., Burian, J., et al., 2010. Fast-neutron dose evaluation in BNCT with Fricke gel layer detectors. Radiat. Meas. 45, 1398–1401.

Ghaseminejad, S., Mesbahi, A., Khajeali, A., Farajollahi, A.R., 2017. Dosimetric evaluation of small IMRT beamlets in the presence of bone inhomogeneity using NIPAM polymer gel and Monte Carlo simulation. Radiat. Meas. 105, 62–69.

Gifford, K.A., Horton, J.L., Jackson, E.F., Steger, T.R., Heard, M.P., Mourtada, F., et al., 2005. Comparison of Monte Carlo calculations around a Fletcher Suit Delclos ovoid with radiochromic film and normoxic polymer gel dosimetry. Med. Phys. 32, 2288–2294.

Gopishankar, N., Vivekanandhan, S., Kale, S.S., Rath, G.K., Senthilkumaran, S., Thulkar, S., et al., 2012. MAGAT gel and EBT2 film-based dosimetry for evaluating source plugging-based treatment plan in Gamma Knife stereotactic radiosurgery. J. Appl. Clin. Med. Phys. 13, 46–61.

Gopishankar, N., Vivekanandhan, S., Rath, G.K., et al., 2013. Indigenously developed multipurpose acrylic head phantom for verification of IMRT using film and gel dosimetry. J. Appl. Clin. Med. Phys. 14, 62–76.

Govi, N., Gueye, P., Avery, S., 2013. Application of MAGAT polymer gel dosimetry in

breast balloon. J. Phys. Conf. Ser. 444.
Grebe, G., Pfaender, M., Roll, M., Luedemann, L., 2001. Dynamic arc radiosurgery and radiotherapy: commissioning and verification of dose distributions. Int. J. Radiat. Oncol. Biol. 49, 1451–1460.
Guillerminet, C., Gschwind, R., Makovicka, L., Novotny, J., Spevacek, V., Cechak, T., 2003. Determination of 3D dose distribution by PAG and Monte-Carlo simulations. Nucl. Instrum. Methods Phys. Res. B 207, 124–130.
Gustavsson, H., Karlsson, A., Back, S.A., Olsson, L.E., Haraldsson, P., Engstrom, P., et al., 2003. MAGIC-type polymer gel for three-dimensional dosimetry: intensity-modulated radiation therapy verification. Med. Phys. 30, 1264–1271.
Gustavsson, H., Bäck, S.Å.J., Medin, J., Grusell, E., Olsson, L.E., 2004. Linear energy transfer dependence of a normoxic polymer gel dosimeter investigated using proton beam absorbed dose measurements. Phys. Med. Biol. 49, 3847.
Haraldsson, P., Bäck, S., Magnusson, P., Olsson, L., 2000. Dose response characteristics and basic dose distribution data for a polymerization-based dosemeter gel evaluated using MR. Br. J. Radiol. 73, 58–65.
Hayashi, S., Yoshioka, M., Usui, S., Haneda, K., Kondo, T., McAuley, K.B., et al., 2010. A study on the role of gelatin in methacrylic-acid-based gel dosimeters. Radiat. Phys. Chem. 79, 803–808.
Hepworth, S.J., McJury, M., Oldham, M., Morton, E.J., Doran, S.J., 1999. Dose mapping of inhomogeneities positioned in radiosensitive polymer gels. Nucl. Instrum. Methods Phys. Res. A 422, 756–760.
Hill, B., Bäck, S.Å.J., Lepage, M., Simpson, J., Healy, B., Baldock, C., 2002. Investigation and analysis of ferrous sulfate polyvinyl alcohol (PVA) gel dosimeter. Phys. Med. Biol. 47, 4233.
Hill, B., Venning, A., Baldock, C., 2005. The dose response of normoxic polymer gel dosimeters measured using X-ray CT. Br. J. Radiol. 78, 623–630.
Hilts, M., Audet, C., Duzenli, C., Jirasek, A., 2000. Polymer gel dosimetry using x-ray computed tomography: a feasibility study. Phys. Med. Biol. 45, 2559–2571.
Hsieh, C.-M., Leung, J.H., Ng, Y.-B., Cheng, C.-W., Sun, J.-C., Lin, P.-C., et al., 2015. The feasibility assessment of radiation dose of movement 3D NIPAM gel by magnetic resonance imaging. Radiat. Phys. Chem. 116, 142–146.
Hsieh, L.L., Shieh, J.I., Wei, L.J., Wang, Y.C., Cheng, K.Y., Shih, C.T., 2017. Polymer gel dosimeters for pretreatment radiotherapy verification using the three-dimensional gamma evaluation and pass rate maps. Phys. Med. 37, 75–81.
Hurley, C., Venning, A., Baldock, C., 2005. A study of a normoxic polymer gel dosimeter comprising methacrylic acid, gelatin and tetrakis (hydroxymethyl) phosphonium chloride (MAGAT). Appl. Radiat. Isot. 63, 443–456.
Hurley, C., McLucas, C., Pedrazzini, G., Baldock, C., 2006. High-resolution gel dosimetry of a HDR brachytherapy source using normoxic polymer gel dosimeters: preliminary study. Nucl. Instrum. Methods Phys. Res. A 565, 801–811.
Ibbott, G.S., 2004. Applications of gel dosimetry. J. Phys. Conf. Ser. 56, 108.
Ibbott, G.S., Maryanski, M.J., Eastman, P., Holcomb, S.D., Zhang, Y., Avison, R.G., et al., 1997. Three-dimensional visualization and measurement of conformal dose distributions using magnetic resonance imaging of BANG polymer gel dosimeters. Int. J. Radiat. Oncol. Biol. Phys. 38, 1097–1103.
Jirasek, A., Hilts, M., McAuley, K.B., 2010. Polymer gel dosimeters with enhanced sensitivity for use in X-ray CT polymer gel dosimetry. Phys. Med. Biol. 55, 5269–5281.
Kairn, T., Taylor, M.L., Crowe, S.B., Dunn, L., Franich, R.D., Kenny, J., et al., 2012. Monte Carlo verification of gel dosimetry measurements for stereotactic radiotherapy. Phys. Med. Biol. 57, 3359–3369.
Kakade, N.R., Sharma, S.D., 2015. Dose enhancement in gold nanoparticle-aided radiotherapy for the therapeutic photon beams using Monte Carlo technique. J. Cancer Res. Ther. 11, 94–97.
Khadem-Abolfazli, M., Mahdavi, M., Mahdavi, S.R.M., Ataei, G., 2013. Dose enhancement effect of gold nanoparticles on MAGICA polymer gel in mega voltage radiation therapy. Int. J. Radiat. Res. 11, 55–61.
Khajeali, A., Khodadadi, R., Kasesaz, Y., Horsfield, M., Farajollahi, A.R., 2017. Measurement of dose distribution from treatment of shallow brain tumors in BNCT by NIPAM polymer gel. Prog. Nucl. Energy 100, 292–296.
Khan, F.M., Gibbons, J.P., 2014. Khan's the Physics of Radiation Therapy. Lippincott Williams & Wilkins.
Khezerloo, D., Nedaie, H.A., Takavar, A., Zirak, A., Farhood, B., Movahedinejhad, H., et al., 2017. PRESAGE® as a solid 3-D radiation dosimeter: a review article. Radiat. Phys. Chem. 141, 88–97.
Khosravi, H., Hashemi, B., Mahdavi, S.R., Hejazi, P., 2015. Effect of gold nanoparticles on prostate dose distribution under Ir-192 internal and 18 MV external radiotherapy procedures using gel dosimetry and Monte Carlo method. J. Biomed. Phys. Eng. 5, 3–14.
Khosravi, H., Hashemi, B., Rahmani, F., Ebadi, A., 2016. Investigation of the gold nanoparticles effects on the prostate dose distribution in brachytherapy: gel dosimetry and Monte Carlo method. J. Contemp. Brachyther. 8, 422–428.
Khosroabadi, M., Farhood, B., Ghorbani, M., Hamzian, N., Moghaddam, H.R., Davenport, D., 2016. Tissue composition effect on dose distribution in neutron brachytherapy/neutron capture therapy. Rep. Prac. Oncol. Radiother. 21, 8–16.
Kipouros, P., Pappas, E., Baras, P., Hatzipanayoti, D., Karaiskos, P., Sakelliou, L., et al., 2001. Wide dynamic dose range of VIPAR polymer gel dosimetry. Phys. Med. Biol. 46, 2143–2159.
Kipouros, P., Papagiannis, P., Sakelliou, L., Karaiskos, P., Sandilos, P., Baras, P., et al., 2003. 3D dose verification in ^{192}Ir HDR prostate monotherapy using polymer gels and MRI. Med. Phys. 30, 2031–2039.
Koeva, V., Olding, T., Jirasek, A., Schreiner, L., McAuley, K., 2009. Preliminary investigation of the NMR, optical and x-ray CT dose–response of polymer gel dosimeters incorporating cosolvents to improve dose sensitivity. Phys. Med. Biol. 54, 2779.
Kozicki, M., Maras, P., Rybka, K., Biegański, T., 2009. VIPARnd - GeVero® tool in planning of TPS scheduled brain tumour radiotherapy. J. Phys. Conf. Ser. 164.
Kozicki, M., Jaszczak, M., Maras, P., Dudek, M., Cłapa, M., 2017. On the development of a VIPARnd radiotherapy 3D polymer gel dosimeter. Phys. Med. Biol. 62, 986–1008.
Lepage, M., Jayasakera, P., Bäck, S.Å.J., Baldock, C., 2001. Dose resolution optimization of polymer gel dosimeters using different monomers. Phys. Med. Biol. 46, 2665.
Lopatiuk-Tirpak, O., Langen, K.M., Meeks, S.L., Kupelian, P.A., Zeidan, O.A., Maryanski, M.J., 2008. Performance evaluation of an improved optical computed tomography polymer gel dosimeter system for 3D dose verification of static and dynamic phantom deliveries. Med. Phys. 35, 3847–3859.
Low, D.A., Harms, W.B., Mutic, S., Purdy, J.A., 1998. A technique for the quantitative evaluation of dose distributions. Med. Phys. 25, 656–661.
Mann, P., Witte, M., Moser, T., Lang, C., Runz, A., Johnen, W., et al., 2017. 3D dosimetric validation of motion compensation concepts in radiotherapy using an anthropomorphic dynamic lung phantom. Phys. Med. Biol. 62, 573–595.
Marques, T., Schwarcke, M., Garrido, C., Zucolot, V., Baffa, O., Nicolucci, P., 2010. Gel dosimetry analysis of gold nanoparticle application in kilovoltage radiation therapy. J. Phys. Conf. Ser. 250, 418–422.
Marques, T.M., Fernandes, J.F., Barbi, G.B., Nicolucci, P.N., Baffa, O.B., 2009. MAGIC with formaldehyde applied to dosimetry of HDR brachytherapy source. J. Phys. Conf. Ser. 164.
Maryanski, M., Schulz, R., Ibbott, G., Gatenby, J., Xie, J., Horton, D., et al., 1994. Magnetic resonance imaging of radiation dose distributions using a polymer-gel dosimeter. Phys. Med. Biol. 39, 1437.
Maryanski, M., Zastavker, Y., Gore, J., 1996a. Radiation dose distributions in three dimensions from tomographic optical density scanning of polymer gels: II. Optical properties of the BANG polymer gel. Phys. Med. Biol. 41, 2705.
Maryanski, M., Ibbott, G., Eastman, P., Schulz, R., Gore, J., 1996b. Radiation therapy dosimetry using magnetic resonance imaging of polymer gels. Med. Phys. 23, 699–705.
Maryanski, M., Audet, C., Gore, J., 1997. Effects of crosslinking and temperature on the dose response of a BANG polymer gel dosimeter. Phys. Med. Biol. 42, 303.
Maryanski, M.J., Gore, J.C., Kennan, R.P., Schulz, R.J., 1993. NMR relaxation enhancement in gels polymerized and cross-linked by ionizing radiation: a new approach to 3D dosimetry by MRI. Magn. Reson. Imaging 11, 253–258.
Mather, M.L., Whittaker, A.K., Baldock, C., 2002. Ultrasound evaluation of polymer gel dosimeters. Phys. Med. Biol. 47, 1449.
McJury, M., Tapper, P.D., Cosgrove, V.P., et al., 1999. Experimental 3D dosimetry around a high-dose-rate clinical ^{192}Ir source using a polyacrylamide gel (PAG) dosimeter. Phys. Med. Biol. 44, 2431–2444.
Meeks, S.L., Bova, F.J., Maryanski, M.J., et al., 1999. Image registration of BANG® gel dose maps for quantitative dosimetry verification. Int. J. Radiat. Oncol. Biol. Phys. 43, 1135–1141.
Moher, D., Liberati, A., Tetzlaff, J., Altman, D.G., 2009. Preferred reporting items for systematic reviews and meta-analyses: the PRISMA statement. Ann. Intern. Med. 151, 264–269 (w264).
Moutsatsos, A., Petrokokkinos, L., Karaiskos, P., Papagiannis, P., Georgiou, E., Dardoufas, K., et al., 2009. Gamma knife output factor measurements using VIP polymer gel dosimetry. Med. Phys. 36, 4277–4287.
Novotny, J., Spevacek, V., Dvorak, P., Cechak, T., 2001. Energy and dose rate dependence of BANG-2 polymer-gel dosimeter. Med. Phys. 28, 2379–2386.
Novotný Jr, J., Dvorák, P., Spevácek, V., Tintera, J., Novotný, J., Cechák, T., 2002. Medical application of 3-D polymer gel dosemeter evaluated by nuclear magnetic resonance. Radiat. Prot. Dosim. 101, 399–402.
Oldham, M., Baustert, I., Lord, C., Smith, T., McJury, M., Warrington, A., et al., 1998. An investigation into the dosimetry of a nine-field tomotherapy irradiation using BANG-gel dosimetry. Phys. Med. Biol. 43, 1113–1132.
Oldham, M., Siewerdsen, J.H., Kumar, S., Wong, J., Jaffray, D.A., 2003. Optical-CT gel-dosimetry I: basic investigations. Med. Phys. 30, 623–634.
Pantelis, E., Karlis, A., Kozicki, M., Papagiannis, P., Sakelliou, L., Rosiak, J., 2004. Polymer gel water equivalence and relative energy response with emphasis on low photon energy dosimetry in brachytherapy. Phys. Med. Biol. 49, 3495.
Pantelis, E., Baltas, D., Georgiou, E., Karaiskos, P., Lymperopoulou, G., Papagiannis, P., et al., 2006. Dose characterization of the new Bebig IsoSeed® I25. S17 using polymer gel and MRI. Nucl. Instrum. Methods Phys. Res. A 569, 529–532.
Papadakis, A.E., Zacharakis, G., Maris, T.G., Ripoll, J., Damilakis, J., 2010. A new optical-CT apparatus for 3-D radiotherapy dosimetry: is free space scanning feasible? IEEE Trans. Med. Imaging 29, 1204–1212.
Pappas, E., Maris, T., Angelopoulos, A., Paparigopoulou, M., Sakelliou, L., Sandilos, P., et al., 1999. A new polymer gel for magnetic resonance imaging (MRI) radiation dosimetry. Phys. Med. Biol. 44, 2677.
Pappas, E., Seimenis, I., Angelopoulos, A., Georgolopoulou, P., Kamariotaki-Paparigopoulou, M., Maris, T., et al., 2001. Narrow stereotactic beam profile measurements using N-vinylpyrrolidone based polymer gels and magnetic resonance imaging. Phys. Med. Biol. 46, 783.
Pavoni, J., Baffa, O., 2012. An evaluation of dosimetric characteristics of MAGIC gel modified by adding formaldehyde (MAGIC-f). Radiat. Meas. 47, 1074–1082.
Pavoni, J.F., Pike, T.L., Snow, J., DeWerd, L., Baffa, O., 2012. Tomotherapy dose distribution verification using MAGIC-f polymer gel dosimetry. Med. Phys. 39, 2877–2884.
Pianoschi, T., Alva, M., Santanna, M., Baffa, O., Nicolucci, P., 2010. MAGIC-f gel dosimetry for clinical electron beam. J. Phys. Conf. Ser. 250, 012037.
Podgorsak, E.B., 2005. Radiation Oncology Physics. A Handbook for Teachers and Students/EB Podgorsak. International Atomic Energy Agency, Vienna, pp. 657.
Pourfallah, T.A., Allahverdi, M., Alam, N.R., Ay, M.R., Zahmatkesh, M.H., 2009. Differential dose volume histograms of Gamma Knife in the presence of inhomogeneities using MRI-polymer gel dosimetry and MC simulation. Med. Phys. 36,

3002–3012.
Pourfallah, T.A., Allahverdi, M., Zahmatkesh, M.H., 2012. Evaluation of the effects of inhomogeneities on dose profiles using polymer gel dosimeter and Monte Carlo simulation in Gamma Knife. Iran. J. Med. Phys. 9, 1–8.
Ramm, U., Weber, U., Bock, M., Krämer, M., Bankamp, A., Damrau, M., et al., 2000. Three-dimensional BANG™ gel dosimetry in conformal carbon ion radiotherapy. Phys. Med. Biol. 45, N95.
Ravichander, T., Hill, B., Venning, J., Baldock, C., 2006. Head and neck field matching verification using three dimensional PAGAT polymer gel dosimetry. J. Phys. Conf. Ser. 56, 286–288.
Sathiyaraj, P., Samuel, J.J., 2018. Dose rate and energy dependence study of methacrylic acid gelatin tetrakis (hydroxymethyl) phosphonium chloride gel with flattened and unflattened photon beams. J. Cancer Res. Ther. 14, 287–291.
Sedaghat, M., Bujold, R., Lepage, M., 2011a. Investigating potential physicochemical errors in polymer gel dosimeters. Phys. Med. Biol. 56, 6083.
Sedaghat, M., Bujold, R., Lepage, M., 2011b. Severe dose inaccuracies caused by an oxygen-antioxidant imbalance in normoxic polymer gel dosimeters. Phys. Med. Biol. 56, 601.
Sellakumar, P., James Jebaseelan, Samuel, E., 2010. Study on energy dependence of PAGAT polymer gel dosimeter evaluated using X-ray CT. Radiat. Meas. 45, 92–97.
Senden, R.J., De Jean, P., McAuley, K.B., Schreiner, L.J., 2006. Polymer gel dosimeters with reduced toxicity: a preliminary investigation of the NMR and optical dose-response using different monomers. Phys. Med. Biol. 51, 3301–3314.
Shih, T.-Y., Yen, T.-H., Liu, Y.-L., Luzhbin, D., Wu, J., 2017. Evaluation of characteristics of high-energy electron beams using N-isopropyl-acrylamide gel dosimeter. Radiat. Phys. Chem. 140, 379–382.
Sigma-Aldrich, 2013a. Acrylamide. Safety data sheet.
Sigma-Aldrich, 2013b. N-Isopropylacrylamide. Safety data sheet.
Sigma-Aldrich, 2014. 2-Acrylamido-2-methyl-1-propanesulfonic acid. Safety data sheet.
Silveira, M.A., Pavoni, J.F., Baffa, O., 2017. Three-dimensional quality assurance of IMRT prostate plans using gel dosimetry. Phys. Med. 34, 1–6.
Tanha, K., Mahdavi, S., Geraily, G., 2014. Comparison of CCC and ETAR dose calculation algorithms in pituitary adenoma radiation treatment planning; Monte Carlo evaluation. J. Radiother. Prac. 13, 447–455.
Toossi, M.T.B., Toossi, M.H.B., Safaeian, G., Hashemian, A., Bayani, S., 2009. Application of MRI normoxic polymer gel dosimetry for the evaluation of radiation dose distribution in external beam radiotherapy. In: Dössel, O., Schlegel, W.C. (Eds.), World Cong. Med. Phys. Biomed. Eng., vol 25/1. Springer, Berlin, Heidelberg, pp. 72–75.
Trapp, J.V., Back, S.A., Lepage, M., Michael, G., Baldock, C., 2001. An experimental study of the dose response of polymer gel dosimeters imaged with x-ray computed tomography. Phys. Med. Biol. 46, 2939–2951.
Trapp, J.V., Partridge, M., Hansen, V.N., et al., 2004. The use of gel dosimetry for verification of electron and photon treatment plants in carcinoma of the scalp. Phys. Med. Biol. 49, 1625–1635.
Uusi-Simola, J., Savolainen, S., Kangasmaki, A., Heikkinen, S., Perkio, J., Ramadan, U.A., et al., 2003. Study of the relative dose-response of BANG-3^{R} polymer gel dosimeters in epithermal neutron irradiation. Phys. Med. Biol. 48, 2895–2906.
Uusi-Simola, J., Heikkinen, S., Kotiluoto, P., Serén, T., Seppälä, T., Auterinen, I., et al., 2007. MAGIC polymer gel for dosimetric verification in boron neutron capture therapy. J. Appl. Clin. Med. Phys. 8, 114–123.
Vandecasteele, J., Ghysel, S., Baete, S., De Deene, Y., 2011. Radio-physical properties of micelle leucodye 3D integrating gel dosimeters. Phys. Med. Biol. 56, 627.
Venning, A., Healy, B., Nitschke, K., Baldock, C., 2005a. Investigation of the MAGAS normoxic polymer gel dosimeter with Pyrex glass walls for clinical radiotherapy dosimetry. Nucl. Instrum. Methods Phys. Res. A 555, 396–402.
Venning, A., Nitschke, K., Keall, P., Baldock, C., 2005b. Radiological properties of normoxic polymer gel dosimeters. Med. Phys. 32, 1047–1053.
Waldenberg, C., Hauer, A.K., Gustafsson, C., Ceberg, S., 2017. Dose integration and dose rate characteristics of a NiPAM polymer gel MRI dosimeter system. J. Phys. Conf. Ser. 847, 012063.
Watanabe, Y., Kubo, H., 2011. A variable echo-number method for estimating R_2 in MRI-based polymer gel dosimetry. Med. Phys. 38, 975–982.
Watanabe, Y., Mooij, R., Perera, G.M., Maryanski, M.J., 2004. Heterogeneity phantoms for visualization of 3D dose distributions by MRI-based polymer gel dosimetry. Med. Phys. 31, 975–984.
Wojnecki, C., Green, S., 2001. A computational study into the use of polyacrylamide gel and A-150 plastic as brain tissue substitutes for boron neutron capture therapy. Phys. Med. Biol. 46, 1399–1405.
Wuu, C.S., Xu, Y., 2006. Three-dimensional dose verification for intensity modulated radiation therapy using optical CT based polymer gel dosimetry. Med. Phys. 33, 1412–1419.
Wuu, C.S., Schiff, P.B., Maryanski, M., Liu, T., Borzillary, S., Weinberger, J., 2002. 3D dosimetry study of ^{188}Re liquid balloon for intravascular brachytherapy using BANG polymer gel dosemeters. Radiat. Prot. Dosim. 99, 397–400.
Wuu, C.S., Schiff, P., Maryanski, M.J., Liu, T., Borzillary, S., Weinberger, J., 2003. Dosimetry study of Re-188 liquid balloon for intravascular brachytherapy using polymer gel dosimeters and laser-beam optical CT scanner. Med. Phys. 30, 132–137.
Wuu, C.-S., Xu, Y., 2011. 3-D dosimetry with optical CT scanning of polymer gels and radiochromic plastic dosimeter. Radiat. Meas. 46, 1903–1907.
Xu, Y., Wuu, C.S., Maryanski, M.J., 2004. Performance of a commercial optical CT scanner and polymer gel dosimeters for 3-D dose verification. Med. Phys. 31, 3024–3033.
Yao, C.H., Chang, T.H., Tsai, M.J., Lai, Y.C., Chen, Y.A., Chang, Y.J., et al., 2017. Dose verification of volumetric modulation arc therapy by using a NIPAM gel dosimeter combined with a parallel-beam optical computed tomography scanner. J. Radioanal. Nucl. Chem. 311, 1277–1286.
Yoshioka, M., Hayashi, S., Usui, S., Haneda, K., Kondo, T., Numasaki, H., et al., 2010. Improved dose sensitivity of normoxic polyacrylamide gelatin gel dosimeter with sucrose. J. Phys. Conf. Ser. 250, 012016.
Zehtabian, M., Faghihi, R., Zahmatkesh, M.H., et al., 2012. Investigation of the dose rate dependency of the PAGAT gel dosimeter at low dose rates. Radiat. Meas. 47, 139–144.
Zeidan, O., Sriprisan, S., Lopatiuk-Tirpak, O., Kupelian, P., Meeks, S., Hsi, W., et al., 2010. Dosimetric evaluation of a novel polymer gel dosimeter for proton therapy. Med. Phys. 37, 2145–2152.